

The relation between hydraulic conductivity, soil characteristics and macrofossil analysis, accompanied by pedological memory analysis of microforms in boreal peatlands

Author:

Edward van Westrene

Supervisors:

Jelmer Nijp

Arnaud Temme

Elisabet Bohlin

The relation between hydraulic conductivity, soil characteristics and macrofossil analysis, accompanied by pedological memory analysis of microforms in boreal peatlands

Author: Edward van Westrene

Registration number: 901013-946-040

Course code: SGL-80439



Supervisors:

Jelmer J. Nijp¹, Arnaud J.A.M. Temme¹⁺² and Elisabet Bohlin³

¹ Soil Geography and Landscape Group, Wageningen University, Wageningen, The Netherlands

² Department of Geography, Kansas State University, Manhattan, KS, USA

³ Department of Forest Ecology and Management, Swedish University of Agricultural Sciences, Umeå, Sweden

Final version

Wageningen University, Wageningen, the Netherlands.

08/10/2017

Abstract

Feedbacks between soil, vegetation and hydrological properties result in spatial vegetation patterns in peatland ecosystems. This study quantifies the gradient of an important property influencing the hydrological functioning of peatlands, the saturated hydraulic conductivity (K_{sat}), over depth for different spatial patterns (microforms), whereby the drier microforms (hummocks) have a lower K_{sat} value compared to wetter microforms (hollows) for the first 60 cm depth. Furthermore, the relationship between the K_{sat} and the decomposition degree (von Post), bulk density and water content is researched, wherein only the von Post had a significant effect on the K_{sat} . A novel part of this research is the relationship between the size and pattern type of the microforms. Statistical model outcome showed that the minimal size and the area size of a microform influence the K_{sat} . Since vegetation is the main driver of the differences in microforms, the influence of the botanical composition of plant remains in peat (macrofossils) on the K_{sat} was researched. Only the von Post scale, the water content and the type of pattern could explain 11.9% of the macrofossil composition. Macrofossil composition was used to see whether microforms were persistent in depth and possibly larger microforms were more persistent for changes. Large hollows were more constant in depth, compared to the small hollow vegetation, but hummocks not significantly. Macrofossil analysis of individual cores gave insight in the variation of the macrofossil composition or pedological memory (persistence). There is a lot of spatial variation in peatlands in terms of macrofossils.

Keywords: peatlands, microform, saturated hydraulic conductivity, pedological memory, macrofossils, climate change.

Table of Contents

Abstract	iii
1. Introduction	1
2. Research Questions and Hypotheses	3
1.) Is there a K_{sat} gradient over depth, and is there a difference for different microforms?	3
1a) Is there a vertical K_{sat} gradient over depth?	3
1b) Is there a difference in K_{sat} between hummocks and hollows?	3
2.) How is the K_{sat} related to hydrophysical characteristics, botanical composition and microform size characteristics?	3
2a) How are K_{sat} values related to hydrophysical properties?	3
2b) What is the relation between peat botanical composition and hydrophysical characteristics?	3
2c) Do the type and surface area of microform patterns influence K_{sat} ?	3
3.) Is pedological memory visible in the macrofossil composition of microforms in peatlands?	3
3a) Do large microforms have higher similarity in macrofossil composition over depth than smaller microforms?	3
3b) What is the similarity of individual peat cores?	4
3. Methods and Materials	5
3.1. Site description and sampling design	5
3.2. Measurements	6
3.2.1. Experimental setup	6
3.2.2. Hydraulic conductivity	6
3.3. Peat core collection	7
3.3.1. Macrofossils	7
3.3.2. Environmental variables	8
3.4. Microform size and type determination	8
3.4.1. Photographs	8
3.4.2. Aerial image	8
3.4.3. Pattern type	8
3.4.4. Data creation	9
3.5. Data analysis	10
3.5.1. Hydraulic conductivity	10
3.5.2. Pedological memory data	11
3.5.3. Statistics	11
4. Results	13
4.1. K_{sat} gradient over depth and differences between microforms	13
1a) Is there a vertical K_{sat} gradient over depth?	13
1b) Is there a difference in K_{sat} between hummocks and hollows?	14
4.2. K_{sat} in relation to other (environmental) variables and the predictive power of environmental variables on macrofossil composition	15
2a) How are K_{sat} values related to other environmental variables?	15
2b) Relation between peat botanical composition and hydrophysical characteristics	17
2c) Do the type and surface area of microform patterns influence K_{sat} ?	19
4.3. Pedological memory in peatland microforms	21

3a)	Do large microform have higher similarity than smaller microforms, in terms of macrofossils?	21
3b)	Pedological memory per site	24
	Diagnostic diagram of the macrofossils after cluster analysis	Error! Bookmark not defined.
5.	Discussion	26
5.1.	K_{sat} gradient over depth and differences between microforms	26
5.2.	K_{sat} in relation to other (environmental) variables?	26
2a)	How are K_{sat} values related to other environmental variables and how can environmental variables explain variation in macrofossils?	26
2b)	Do the type and surface area of microform patches influence K_{sat} ?	27
5.3.	Pedological memory in peatland microforms.....	27
3a)	Do large microform have higher similarity than smaller microforms, in terms of macrofossils?	27
3b)	Do individual cores show pedological memory?	27
3c)	Limitations.....	28
6.	Conclusion	29
6.1.	K_{sat} gradient over depth and differences between microforms	29
6.2.	K_{sat} in relation to other (environmental) variables?	29
6.3.	Pedological memory in peatland microforms.....	29
7.	Recommendations	30
7.1.	Data collection in the field.....	30
7.2.	Macrofossil prediction model.....	30
7.3.	Macrofossil in terms of hummock or hollow ratio	30
7.4.	Further research.....	30
8.	Acknowledgements	31
	References	32
	Appendix.....	I
	Remarks and copyright images	I
	Pycnometer table	I
	Diagnostic diagram of the macrofossils after cluster analysis	II
	Reference measurements for the K_{sat} correction.....	VI
	Parameters for the deviance values of the microform types.....	VI
	PCA and RDA analyses	VIII
	Correlation data.....	IX

1. Introduction

Only 2.6% of the terrestrial surface is occupied by peatlands (Joosten & Clarke, 2002). This ostensibly small part represents 30% of the total terrestrial carbon pool (Gorham, 1991). If this amount of carbon ended up in the atmosphere as CO₂, the concentrations would be doubled to around 800 ppm (Dlugokencky & Tans, 2016). Recent studies suggest that local increase of CO₂ emissions has a significant direct influence on atmospheric circulation and therefore on global precipitation changes (Collins *et al.*, 2013a). Northern peatlands (>45 °N) are closely linked with feedbacks to the global climate system (Bridgham *et al.*, 2008; Frohling & Roulet, 2007). It is projected that climate change will cause an increase of the yearly sum of rainwater in northern peatlands (Collins *et al.*, 2013b). Rain events will be more intense, but there will be fewer events (Collins *et al.*, 2013b), resulting in longer and more frequent droughts in these peatlands. Drought has a large negative impact on the growth of peat moss and can thereby reduce the carbon sequestration (Alm *et al.*, 1999; Bragazza, 2008; Nijp *et al.*, 2014). Therefore concern has risen that peatlands may switch from sinks to sources of atmospheric carbon under changing climate (Yu *et al.*, 2010).

A key component for the carbon sequestration in peatlands is the distance between the peat surface and the groundwater level (GWL) (Belyea & Malmer, 2004). Height differences between the surface and the groundwater level are a key determinant of plant species distribution (Malmer, 1962). Numerous feedback mechanisms between vegetation and height differences, result in distinct microforms in peatlands (Belyea & Clymo, 2001). The microform closest to the groundwater, a hollow, will have no or a very small acrotelm (the layer of aerobic peat). The microform farthest to the groundwater, a hummock, will have a thicker acrotelm above the catotelm (the layer of anaerobic peat) (Alm *et al.*, 1999; Eppinga *et al.*, 2009a). An important inhibitor of plant growth in peatlands is water stress. Water stress occurs when there is a relatively high water level because of waterlogging. On the other hand, a relatively low water level causes desiccation, which also results in water stress (Ridolfi *et al.*, 2006). Optimal peat growth will occur at intermediate acrotelm thickness (Eppinga *et al.*, 2009a). Plant growth will eventually result in organic matter sequestration: a positive feedback between the net rate of peat formation and acrotelm thickness, mainly because of increased production of vascular plants (Belyea & Clymo, 2001). This feedback mechanism is an explanation of how peatland microforms may develop either into a wet, sparsely vegetated, low-productive state, or a dry, densely vegetated high-productive state (Eppinga *et al.*, 2009a). Slight differences between wetter and drier sites may eventually amplify and result in spatial patterns of sharply bounded microforms (Eppinga *et al.*, 2009a). Different types of vegetation lead to differences in productive state and thereby hydrology and peat accumulation (Eppinga *et al.*, 2009b). Plants adapt to their environment and change their environment through feedbacks, therefore plants and their buried remains (macrofossils) can be seen as an important indicator of habitat conditions (Rydin *et al.*, 2013). Another type of feedback is the convective transport of nutrients in groundwater toward areas with higher vascular plant biomass, driven by differences in transpiration. This feedback mechanism is able to explain regular string - and maze patterns in peatlands (Rietkerk *et al.*, 2004a). When plant productivity is limited by nutrient flow, these feedback mechanisms may lead to self-organized patchiness such as observed string patterns on slopes and maze patterns on flat ground (Rietkerk *et al.*, 2004b). Next to nutrient accumulation, water ponding and peat accumulation are structuring mechanisms for peatland patterning (Eppinga *et al.*, 2009a). Water ponding will occur when the water cannot infiltrate as a result of lower hydraulic conductivity, water may accumulate upslope of a hummock, stimulating the formation of hollows (Eppinga *et al.*, 2009a). That the water ponding mechanism can result in hummock and hollow patterning on peatland slopes, is shown in models (Arens, 2017; Couwenberg, 2005; Couwenberg & Joosten, 2005; Swanson & Grigal, 1988). Nutrient transport and water ponding are mainly regulated by the hydraulic conductivity.

Positive feedback between vegetation and limited water and nutrient supply is considered the principal underlying catastrophic ecosystem shift (Rietkerk & van de Koppel, 1997; Scheffer *et al.*, 2001; Scheffer & Carpenter, 2003). A catastrophic ecosystem shift is an abrupt switch to a contrasting alternative stable state (Scheffer *et al.*, 2001). This can cause a heterogeneous microform pattern to collapse into a homogenous microform. When this shift occurs it becomes harder to return to the original heterogeneous state (hysteresis). A homogenous microform would result in a decrease of biodiversity, change in hydrology, difference in carbon storage and no resilience of an ecosystem to climate change.

Pedological memory is present as the location of plants is influenced by past locations of plants, via the effect of plants on soil properties (Phillips & Marion, 2004). It is expected that pedological memory plays an important role in the relationship between microform location and soil morphology. In peatlands, a large pedological memory occurs when the previous surface vegetation, transformed in peat, influences the hydraulic structure of peat after younger peat layers buried it. This can be revealed by pillars of a microform having the same hydraulic conductivity characteristics (Baird *et al.*, 2016), where hummocks have a lower saturated hydraulic conductivity compared to hollows (Morris *et al.*, 2015; Swanson & Grigal, 1988). Paleo-ecological studies have revealed that microtopography of hummocks and hollows can persist for thousands of years (Moore, 1977). Microforms are remarkably resilient to changes in environment conditions, such as climate change (Belyea & Clymo, 2001; Nungesser, 2003). However, this resilience is lost when changes in climate pass environmental thresholds. Then peatland will be dominated by different microstructures (Belyea & Malmer, 2004) indicating that a catastrophic shift has occurred. Individual microforms can persist on the same location for hundreds, or even thousands of years (Aaviksoo *et al.*, 1993; Barber, 1981; Walker & Walker, 1961). On the other

hand, more recent research shows that the persistence of a microform is more in the order of 10 to 100 years' time (El-Daoushy *et al.*, 1982; Malmer & Wallén, 2004; Wieder, 2001). The different timespans are in contrast with the previous older studies.

Despite the importance of microforms, little data is available and little research is performed on the physical and hydrological properties that are different for microforms (Belyea & Baird, 2006). Changes of hydrophysical properties with depth and interaction with decomposition and other parameters are still unclear (Morris *et al.*, 2012). For the first research question the focus will be on the K_{sat} and depth relation, since the K_{sat} is an important hydrophysical parameter and can vary over depth (Price *et al.*, 2003). Also different microforms are important for patterns in peatland. There could be a difference in K_{sat} for hummocks and hollows like in Whittington *et al.* (2007). It is essential to know whether the K_{sat} is an important parameter that drives peatland hydrology and microform patterns. If so, it would be of great value to know which factors influence this parameter. Morris *et al.* (2015) showed that the depth of the sample, the type of microform (hollow/hummock) and whether the sampling location was flat or on a slope, played a role in the K_{sat} . To add to Morris *et al.* (2015), the same and other environmental variables are used to predict the K_{sat} to determine relations between hydrophysical parameters. In addition, the relationship between hydrophysical parameters and the macrofossils is explored. And the relation between the K_{sat} and microform characteristics for instance the different sizes of the microform and pattern type could serve as a proxy for the K_{sat} . The macrofossils can also provide valuable information on the plant composition in the past and thereby information about catastrophic shifts and the resilience of the microforms.

It is essential to gain more insight in the mechanisms beyond microform patterns (Morris *et al.*, 2013; Swanson & Grigal, 1988), to improve e.g. monitoring programs and prevent unwanted catastrophic shifts from heterogeneous peatlands into homogenous peatlands.

2. Research Questions and Hypotheses

1.) Is there a K_{sat} gradient over depth, and is there a difference for different microforms?

1a) Is there a vertical K_{sat} gradient over depth?

It is hypothesized that the K_{sat} will have an exponential decline over depth. Peatland surface structure (i.e., vegetation composition, acrotelm thickness) and developmental topography (i.e., catotelm thickness) are linked to hydrology (Belyea & Malmer, 2004). Hydraulic conductivity is relatively high in poorly decomposed litter near the vegetation surface, but declines as the material becomes more decomposed in its transition to peat (Boelter, 1969; Hoag & Price, 1995). Furthermore, Ingram (1983) wrote: "It is expected that the hydraulic conductivity (K_{sat}) declines with increasing depth (or decomposition)."

1b) Is there a difference in K_{sat} between hummocks and hollows?

A lower K_{sat} value is expected for hummocks compared to hollows. If the K_{sat} values over depth are lower, the differences between the microforms could become smaller. At greater depth the soil is compressed and the distance between the current vegetation becomes shorter, thereby the differences between the microforms are less profound. In Branham and Strack (2014) is stated that Ivanov (1975) suggested that K_{sat} is at least an order of magnitude greater in wet (hollow) microforms compared with dry (hummock) microforms.

2.) How is the K_{sat} related to hydrophysical characteristics, botanical composition and microform size characteristics?

2a) How are K_{sat} values related to hydrophysical properties?

Next to depth, other hydrophysical properties could influence the K_{sat} . It is expected that the von Post negatively influence the K_{sat} . With a higher von Post value the soil is more decomposed and clotted together, lowering the K_{sat} . In addition, the bulk density also negatively influences the K_{sat} . Soil with a higher bulk density possibly has fewer pores and a higher solid fraction, thereby lowering the K_{sat} . For the water content, a positive relationship is expected in relation to the K_{sat} . If more water can stay in the soil, there is a higher chance of a higher hydraulic conductivity. The bulk density and von Post shows the same relationship in respect to the K_{sat} measured in a laboratory by: Branham and Strack (2014).

2b) What is the relation between peat botanical composition and hydrophysical characteristics?

The K_{sat} is an important parameter, therefore possibly able to explain some of the plant species found in the soil. Roots are likely to create channels in the soil influencing the K_{sat} . And different plant species could be more compacted than others, in which the K_{sat} may differ between plants. The von Post is also a parameter which could have a relationship to the botanical composition. Some plant species are more likely to decompose, whereas others could be more resilient resulting in differences in von Post.

2c) Do the type and surface area of microform patterns influence K_{sat} ?

If there is a relationship between the sizes of a microform and K_{sat} , the relationship would be the strongest in the shallowest K_{sat} measurement, since that is most closely related to the current microform. It is expected that a relative large microform has an effect on the K_{sat} compared to a relatively smaller microform. It could be that smaller microforms look more like the other type of microform, whereas the larger microform behaves like the type should do. Furthermore, it is expected that at least minimal size would play a role, since it could be that there is a threshold before the K_{sat} represents the microform. The effect of the other size measurements on the K_{sat} is unknown. Pedological memory in peatland microforms

3.) Is pedological memory visible in the macrofossil composition of microforms in peatlands?

3a) Do large microforms have higher similarity in macrofossil composition over depth than smaller microforms?

It is expected that a big microform has a higher similarity or a lower dissimilarity between plant species over depth, compared to smaller microforms. The larger an object is, the more resilient it is to changes and therefore it is more likely that the plant species change less often.

Macrofossils can be seen as a climate proxy (Barber *et al.*, 2003). Maybe they also serve as proxy for the resilience of a microform over the years (or depth). A larger object has a relatively smaller circumference than a smaller object, making the bigger object possibly more resilient towards changes. Plants that are surrounded by the same plants and plants at the borders of the microform

must compete with different plant species. When the microform is bigger, the ratio of plants surrounded by the plants that prefer the same conditions is larger. It is expected that there is a positive interaction between the size of a microform and similarity of the macrofossil composition in a microform.

3b) What is the similarity of individual peat cores?

Research from the previous century showed that hummocks and hollows may persist for thousands of years (Moore, 1977). Vegetation on hummocks and hollows differ. The vegetation could indicate whether a hummock or hollow persists over depth (time). It is likely that in some locations, pillars of the same kind of vegetation will be found and possibly the smaller microforms do not show hummock/hollow pillars. In that case it acts as proof that smaller microforms have a lower similarity. Individual cores could also show that certain locations have the same plant composition. In that case it is other factors, like type of microform or the spatial orientation in the peatland, that play a role in the plant composition.

3. Methods and Materials

3.1. Site description and sampling design

The research site chosen is highly suitable for this research since it has different microforms of different sizes and different types of microforms. In the middle of the mire is a Flux tower that provides meteorological data. Furthermore, boardwalks are installed throughout the mire and it was possible to build more on desired locations. The boardwalks prevented disturbance of the mire surface and measurements during the field campaign.

Degerö Stormyr, Sweden (64°11' 23.565" N, 19°33' 55.291" E) is a mixed acid mire system of 6.5 km² in the Kulbäcksliden Experimental Forest (270 m.a.s.l.). This forest is located near Vindeln in the county of Västerbotten, between two major rivers, Umeälven and Vindelälven, Northern Sweden, approximately 70 km inland of the Gulf of Bothnia (Figure 1). The mire is a complex system of interconnected smaller mires divided by inlets and ridges of glacial till, containing both bogs and fens. Peat depth varies between 3 and 4 meters, however, with some depressions up to 8 meters depth. These depressions correspond with an age of approximately 8000 years old (Nilsson *et al.*, 2008).

Several vegetation types are found throughout the mire, the distinction between hummocks and hollows is mainly done by looking at distinct vegetation. In the hollow are no trees, only 2.5% of the sites are covered by dwarf shrubs, whereas sedges make up to over 30% and Sphagnum covers 100% of the corresponding layer. *Andromeda polifolia* and occasionally some *Rubus chamaemorus* and *Drosera L.* can be found in the dwarf shrubs layer, whereas sedges are mainly *Eriophorum vaginatum*. The *Sphagnum* layer is divided between *Sphagnum majus* and *Sphagnum balticum* and sometimes *Sphagnum magellanicum* is found. The hummocks are on some occasions inhabited by small trees. This microform contains on average 10% more dwarf shrubs than the hollows, is covered by sedges for less than 15% and the Sphagnum layer covers also for 100%. Small trees of *Betula Nana*, *Calluna vulgaris*, *Rubus chamaemorus*, *Andromeda polifolia* and on rare occasions, lichens are found. The Sphagnum layer mainly consists of *Sphagnum fuscum* followed by *Sphagnum balticum*, *Sphagnum papillosum*, *Sphagnum rubellum* and rarely, *Sphagnum magellanicum* and *Sphagnum lindbergii* were found. Near the edges of the mire, plants of the genus *Calliargon* were found (unpublished data).

The climate is defined as cold temperate humid. Based on data from the closest (4 km north of the measurement site) national reference climate station, Kulbäcksliden (64°6'43.199"N,19°8'2.4"E, altitude 200 m.a.s.l.): the 30-year mean (1961–1990) annual precipitation is 523 mm and mean annual, July and January temperatures based on the same period are respectively +1.2, +14.7 and -12.4 °C (Alexandersson *et al.*, 1991). The length of the growing season, defined as the period in which daily mean temperature exceeds +5 °C (Angstrom, 1974), was 157 ±7 days during each year in the measuring period (2004–2005) (Ottosson-Löfvenius, 2005, 2006). The snow cover normally reaches depths up to 60 cm and lasts for 6 months on average (Nijp *et al.*, 2015; Nilsson *et al.*, 2008).

The growing season rainfall, potential evapotranspiration and temperature for Degerö Stormyr (Table 1)(Nijp *et al.*, 2015).

Table 1. Rain, potential evapotranspiration (PET) and temperature (T_{air}) during the period of 2001-2011 at Degerö Stormyr. Rain and PET values represent mean monthly amounts (mm) ± standard deviations, T_{air} is mean air temperature. In this study the growing season is defined as the period from 15 May until 15 October (Nijp *et al.*, 2015).

Period of the year	Rain (mm)	PET (mm)	T _{air} (°C)
May	43 ±21	100±10	7.4±1.4
June	60±23	120±18	12±1.8
July	99±50	116±11	15±1.3
August	105±55	88±9.7	1.3±1.6
September	79±47	43±4.5	8.0±1.3
October	51±32	16±2.3	1.7±2.0
Growing season	397±83	432±30	9.9±1.6

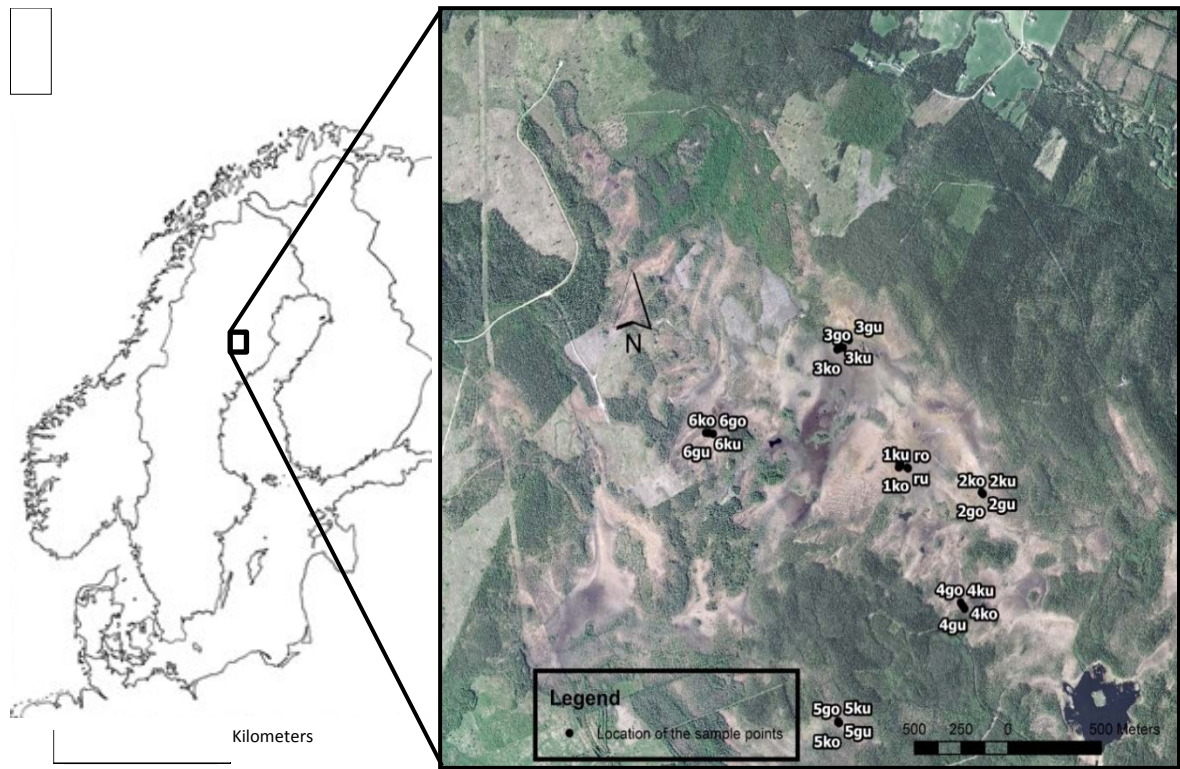


Figure 1. Left: Map of Scandinavia, on which the box (not on scale) represents the location of the field site. Right: Aerial image of the study area, the black dots are the sample location with the site code. (1gu & 1go are next to 1ku & 1ko, but not visible on this image)

3.2. Measurements

3.2.1. Experimental setup

The measurement sites are distributed to give representable results of the mire, via a spatial stratified sampling design (indicated by black dots in Figure 1). The mires will be divided into 6 research sites on which 4 different strata are selected (1 small hummock, 1 large hummock, 1 small hollow and 1 large hollow). The strata will be selected near each other (max. 15 meters). In the strata, a measurement was done in the middle of a microform to get the most representative location. Figure 1 shows the abbreviations starting with the site number, followed by the size (g = large, k=small) and the type of microform (u = hummock, o=hollow). The abbreviations ro and ru are the reference sites for the hydraulic conductivity measurements.

The hummock and hollows were defined mainly based on the current vegetation of the microform. The vegetation is divided in four layers; the tree, dwarf shrub, sedges and the Sphagnum layer. Per layer the cover of different plant species is determined to get the plant cover (%), this to make the best distinction between the two types of microforms. The size selection was based on the local size of the microform. The microforms had to lay in close proximity, but should differ in size (minimal size, L_{est} in section 3.4)

3.2.2. Hydraulic conductivity

The horizontal K_{sat} of the catotelm was measured in-situ by a slug test. This method has proven itself in the field and is relatively simple and inexpensive (Nijp, 2015). A piezometer is inserted in a pre-augured hole in the peat, a known amount of water is rapidly added to the piezometer, which creates a hydraulic head difference and hence the water will flow from the tube into the peat matrix. By measuring the evolution of the hydraulic head over time with a pressure transducer inside the piezometer tube, an estimation of the K_{sat} can be derived. Each microform was sampled at 10, 30, 60, 100, 150 cm with respect to the (summer) groundwater level (GWL). An exponential decline in K_{sat} could be present over depth, therefore there are more measurements at shallow depth in relation to the amount at greater depth. Before the piezometer was placed a greater depth, it was made sure that there was no difference in pressure between the piezometer and surrounding GWL. The stabilisation time depended on the measurement depth and varied between half a day for the most permeable peat layers to a week for deeper, more impermeable peat layers.

The piezometers consist of PVC tubes (outer diameter 4.0 cm) in which a filter was placed over a length of 10.0 cm, 7.0 cm from the end of the tube to enhance stability. The filter was constructed by drilling holes (diameter 0.8 cm, 41.6% perforation of the total filter surface) in the piezometer and covered with a nylon cloth to prevent clogging of the filter. The bottom of the

piezometers was closed watertight with a cap. Time series of water pressure were obtained using two types of pressure transducers (TD Divers DI240, Van Essen Instruments and LEVEL TROLL 700 water level loggers, In-Situ Europe) with an interval of 5 seconds in the most permeable peat, while 15 seconds was used in the more impermeable peat layers.

The filter of the piezometer was placed at the specified depths with respect to the groundwater level. The groundwater level was chosen as a reference, since the elevation depends on microform, making it harder to compare different microforms.

3.3. Peat core collection

To reconstruct the historical development of the microforms and to determine whether microforms persisted over time, cores from the sites were analysed for plant macrofossil remains. This information was related to environmental variables (peat humification degree, dry bulk density and soil porosity) that were also measured, since these variables are important variables (Rydin *et al.*, 2013). Within 20 cm of the piezometer location, one core left of the piezometer and one right of the piezometer were taken to determine these environmental variables and the macrofossil composition (see Figure 2). The cores next to the piezometer were taken after the measurements with the piezometer were done. The distance between the piezometer and the cores was chosen to get undisturbed samples, but to reduce the variability in space. One core was used for the bulk density and water content data and the other core for the humification degree and the macrofossils. Botanical composition is seen as an important property for determining the nature of peat (Rydin *et al.*, 2013). Macrofossils give information about the botanical composition at a certain place and depth. The plant composition can be used to give information about the vegetation history, and hence the pedological memory. The samples for the macrofossils and the samples for the bulk density and water content were put in sealable bags and transported to the Netherlands as quickly as possible. All the material was cleaned thoroughly with cloths and water before a new sample was taken to avoid contamination of the next sample (De Vleeschouwer *et al.*, 2010). All the cores were taken with a Russian corer, which has a semi-circular chamber with an inner diameter of 4.5 cm. Poor recovery in parts of the cores, particularly in the case of fibric peat, meant that not all the required depths could be sampled.

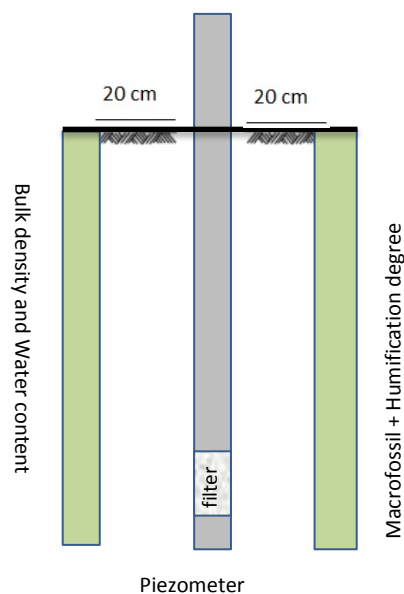


Figure 2. Schematic overview of the peat core collection and piezometer (side view).

3.3.1 Macrofossils

The samples over 10 cm were mixed, this was done to correlate the results with the measured K_{sat} value of which the filter also had a length of 10 cm. The analysis is done using the point count method (Bohlin, 1993), adapted from (Heikurainen & Huikari, 1952). The peat samples were boiled with 10% KOH, then sieved (0.050 mm), mounted with glycerol on a microscopic slide and examined at 100x magnification to species level or section level at least following (Bohlin, 1993). Macrofossil determination was done following (Bohlin, 1993), (Mauquoy & Van Geel, 2007), (Laine *et al.*, 2009) and (Smith & Smith, 2004). The *Sphagna Palustre* section is called *Sphagna Sphagnum* section in the newest taxonomy regulations (Laine *et al.*, 2009), however in this report the old name was used.

3.3.2 Environmental variables

The humification degree was determined in the field using the von Post scale (von Post, 1922). The 10 cm layers were classified with the use of the von Post humification scale, ranging from H1 (undecomposed) until H10 (decomposed). To compare the von Post values with other studies, an expert (Elisabeth Bohlin) accompanied our fieldwork. The determination was always done by the same person (E.C.B. v. Westrene) to guarantee consistency.

A sample of 2 cm in length was taken from the Russian corer to determine the bulk density and the water content in the lab. When the colour and texture was different within the 10 cm, two 2 cm samples were taken and averaged. The same depths were taken as for the conductivity measurements, to correlate the results. The samples were measured for the water content and bulk density, since both environmental variables are easily measurable (De Vleeschouwer *et al.*, 2010). The water content is a percentage (%), determined from the wet weight minus the dry weight and divided by the wet weight. The bulk density is the dry weight divided by the volume of the sample (g/cm^3). A known volume of peat has to be taken and weighed before and after being in an oven at 100°C (Chambers *et al.*, 2010; Hossain *et al.*, 2015). However, in this study a temperature of 70°C was used for 48 h, in order to reduce the risk of burning organic matter (Nijp, 2015). After 48 hours, the weight of the samples did not change anymore, showing a steady state for this temperature (not shown in this report).

After determination of the water content and the bulk density, the particle density was measured using a pycnometer. The air pycnometer measured the volume of the peat sample that was not gas. Measurements were done by: Arens (2017). However, the results (see Table 9 in appendix) showed a lot of variation for each replica and minor variation for different sites and depth, whereby was decided that the measurement error of the pycnometer was too large with respect to the values of the sample itself. An average value for the soil porosity of all the samples was taken, $1.59 (\text{g}/\text{cm}^3)$. By knowing the particle density and the bulk density, the soil porosity was calculated following (Nimmo, 2004), (see eq.1)

$$\phi = 1 - \rho_b / \rho_p \quad (\text{eq.1})$$

Where ϕ , is the soil porosity (-), ρ_b is the bulk density (g/cm^3) and ρ_p is the particle density (g/cm^3). The soil porosity was only used to correct the diver data, see chapter 3.5.1.

3.4. Microform size and type determination

The size of a microform can be a proxy for the K_{sat} . To test this assumption, the microforms in which the peat cores are collected are measured (see Figure 1) and the pattern type of the microforms is determined. The size was determined via photographs which were converted into a orthophoto which was measured. For the large microforms, photographs could not produce a reliable result. In that case an aerial image was used to determine the size of the microform.

3.4.1 Photographs

Photographs of the microforms had to be taken in the field with the same focus on the object. The pictures were taken with a Panasonic DMC-LF1 camera, (4000 x 3000 pixels), a 28 mm F/2.8 lens was used. The ISO-value was set to 80. To capture the peat surface elevation, overlap of the pictures was at least 50% and about 100 photographs were taken per site mostly on 16/07/2016.

3.4.2 Aerial image

In cases when it was not possible to provide a size with the use of the photographs taken in the field, a high resolution (0.5m) aerial image (provided by: Lantmäteriet, Sweden) was imported into ArcGIS including the sampling points, made in the field with an accuracy of 2 meters. The size of the different microforms was measured in ArcGIS (version 10.2.1) in the same way as was done with the orthophotos, see Figure 4.

3.4.3 Pattern type

Eppinga *et al.* (2009a) suggested that the type of pattern could have been the result from different feedbacks. Therefore, sample locations were chosen with different pattern types (maze, string or dotted patterns). The type of pattern was visually determined in the field, see Figure 3 for examples of the patterns. The pattern type would be considered as a variable, possibly lead to different K_{sat} values or other properties.

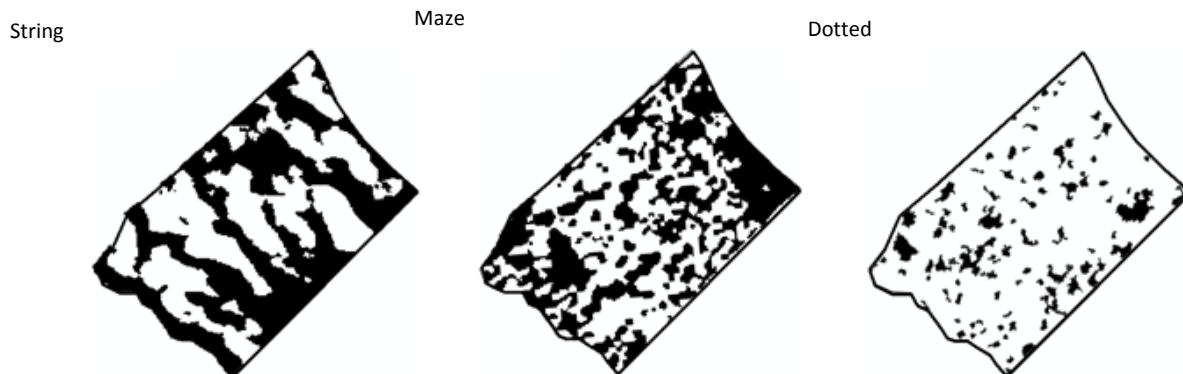


Figure 3. Type of patterns. Black and white represent the hummock and hollows. On the left string patterns, in the middle maze patterns and on the right dotted patterns are visible. Made by: Arens (2017).

3.4.4. Data creation

For the size determination of all the microforms used in the six sites, the following sizes were derived: the minimal length, the maximal length, the total surface and the perimeter of the microform, as well as the minimal length as estimated in the field. The sizes were measured to correlate other variables to the sizes and determine if there is a correlation.

The minimal length (L_{min}) (m) is the minimal length of the microform in order to meet another microform. The maximal length (L_{max}) (m) is the maximal length of the microform to meet another microform. The total surface (A_{total}) (m^2) is the surface of the microform. The perimeter (L_{per}) (m) is the perimeter of the microform. In the field, an estimate (L_{est}) (m) was done of the minimal length in the middle of the microform where it would meet another microform. A schematic representation is provided in Figure 4.

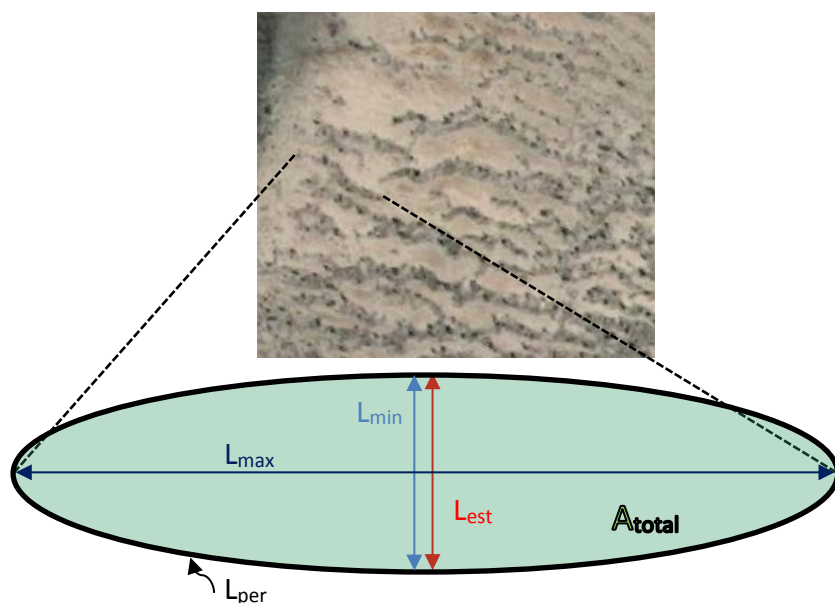


Figure 4. Schematic overview of the size measurements on a microform.

Microforms size was determined based on orthophotos. These were constructed in the program Agisoft, Photoscan Professional (v.1.1.6.). The photographs were aligned to create a sparse point cloud, via the options medium and the option no pair selection. A number of markers (at least 3) were created in the software program and the distance between the markers was scaled preferably in the x, y and z directions, this to calibrate the different photographs with each other. There is an error introduced by the Photoscan Program since it is not able to align the photos 100% correct. During the process, it was made sure that the error stayed at a minimum. In some cases, it happened that one of the three markers had a maximum error of 2 cm on 50 cm (4%) in one (x, y or z) direction. A dense point cloud was created at medium quality, after which a mesh was created followed by a texture product. The result was an orthophoto of the microform, which was exported to ArcGIS.

The orthophotos in ArcGIS were not Georeferenced, therefore the distance between different markers in the orthophoto were related to the measured distance between the markers in the field to get useful measurements for the microform size variables (L_{max} , L_{min} , L_{per} and A_{total}).

For some orthophotos it was not possible to determine the maximal size of the microform due to the large extent of the microforms. In such cases, the size determined using the aerial image was chosen. In all other cases, the size determined by the orthophoto was taken as most representative. The sizes determined via the aerial image did not need the Photoscan software, but could be measured directly.

3.5. Data analysis

3.5.1. Hydraulic conductivity

An estimation of the K_{sat} is done with the use of the equations 2 and 3 (eq.2 ; eq.3) (Zlotnik *et al.*, 2010). The advantage of this formula with respect to the traditional Bouwer-Rice and Hvorslev method is that the Zlotnik equation can be used in unconfined aquifers. Furthermore, this formula does not overestimate the K_{sat} compared to the other methods (Dijk *et al.*, 2017) and it can be applied to any filter depth, installation depth, aquifer thickness and anisotropy in hydraulic conductivity (Dijk *et al.*, 2017). The only assumption is that the storativity is negligible (Dijk *et al.*, 2017).

$$F_{zgd} = \left(\sum_{i=1}^n \left\{ \cos\left(\beta_i \frac{H}{D}\right) - \cos\left(\beta_i \left(H - \frac{L}{D}\right)\right) \right\} \times K_0\left(\frac{\beta_i r_w^*}{D}\right) / \beta_i K_1\left(\frac{\beta_i r_w^*}{D}\right) \right) / L r_w^* / 2D^2 \quad (\text{eq. 2})$$

Where F_{zgd} is the shape factor, K_0 and K_1 are Bessel functions of third kind and zeroth or first order and $\beta_i = \pi(i-0.5)$, L is the filter length (cm), D is the aquifer thickness (cm), r_w^* is the radius of the well scaled to the anisotropy effect (eq. 3).

$$r_w^* = r_w / \sqrt{K_h / K_v} \quad (\text{eq. 3})$$

The coefficients K_h and K_v represent the horizontal and vertical saturated hydraulic conductivity. See (Zlotnik *et al.*, 2010) for details on the derivation and (Nijp, 2015) for the calculation of F_{zgd} using the R software (Nijp, 2015; Team, 2014).

The pressure in the piezometers were corrected for the air pressure, with the use of the data provided by the meteorological station in the middle of the peatland. The soil porosity is used as a correction for the groundwater level when there is a precipitation event and to account for evaporation. There was no difference between the soil porosity for hummock or hollows (see 3.3.2.). Therefore, a mean value for the soil porosity is used. This soil porosity value is used for all depths and locations as the groundwater fluctuations are only expected to occur near the surface and not in the saturated zone. The divers are corrected via equation 4 by Arens (2017).

$$P = P_i - P_{air} - ((R - ET) / \phi) \quad (\text{eq. 4})$$

Where P is the corrected diver pressure (hPa), P_i is the initial diver pressure (hPa), P_{air} is the barometric pressure (hPa), R is the amount of precipitation (mm), ET is the amount of evaporation (mm) and ϕ is the porosity (-).

To test whether shrink and swell of the peat would influence the K_{sat} measurements, a representative hollow and hummock were chosen in the middle of the catchment, near to the meteorological station (see reference site in Figure 1). K_{sat} measurements were performed on this hummock and hollow at a depth of 30 cm below the groundwater level. The variation in K_{sat} for the reference site in a hollow and hummock does not follow the groundwater level (see Figure 18, in appendix) for the reference measurements. The correlation between the K_{sat} in the hollow and the GWL is -0.265 ($p=0.667$), whereas the correlation between the K_{sat} in the hummock and the GWL is -0.120 ($p=0.880$). Therefore, none of the K_{sat} data was corrected for swell and shrink properties due to groundwater level fluctuations.

It occurred 21 out of 66 times that water was added to the piezometer while stabilization had not yet been completed, see Figure 5. Since the hydraulic conductivity could not be calculated using the method described above, a less conventional method was used: The K_{sat} was calculated from the pressure rise after the piezometer installation. First the water pressure time series was selected from the piezometer installation till the water addition. On this part, a formula (eq.5) is fitted with the form of an exponential variogram.

$$Pressure = C_p \left(1 - \exp\left(-\frac{x}{y}\right) \right) + nugget \quad (\text{eq. 5})$$

Where Pressure is the water level (hPa) measured in the piezometer and C_p is the partial sill.

Since the stabilization was not yet complete, the full curve on which the hydraulic conductivity was calculated, was predicted with this solved formula (eq.5). The full curve was then reversed to get the same type of curve as with the other conductivity calculations. The rest of the calculations are the same as the ones calculated on the conventional slug tests.

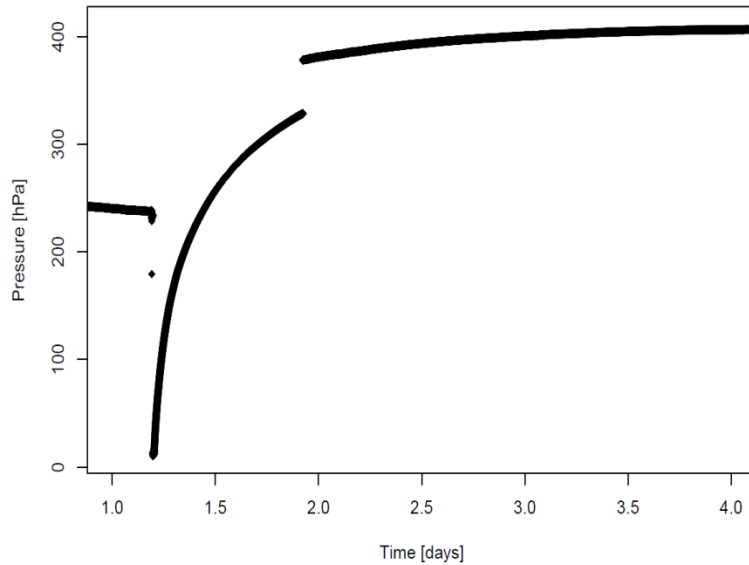


Figure 5. K_{sat} graph when water was added in the case when the stabilization time was not reached. Detail of 5Ko on a depth of 100 cm.

To calculate the gradient of the K_{sat} over depth, the K_{sat} data was fitted against depth via a nonlinear (weighted) least-squares algorithm implemented in R (nls2 function). It was decided to choose this formula with exponential decay of K_{sat} over depth (eq.7).

$$K_{sat} = Ae^{(B-depth)} + C \quad (\text{eq. 7})$$

Where K_{sat} is the hydraulic conductivity, depth is the depth measurement relative to the summer ground water level (cm) and A,B and C are fitting parameters (-).

3.5.2. Pedological memory data

Peat cores were analysed on the macrofossil composition. This data is used as a measure for the pedological memory. A site has a particular macrofossil composition and is compared with the depth of the same core underneath. The absolute distance is calculated over depth using the Manhattan method (eq. 8).

$$d = \sum_{i=1}^n |x_i - y_i| \quad (\text{eq. 8})$$

Where d is the distance measure, n is the number of variables, x_i and y_i are the values of the i th variable, at points x and y respectively. The distance measure was then averaged per microform type (hummock/hollow) and relative size (big/small).

The distance measure was renamed to deviance value. This deviance value was then fitted for eq. 9. The deviance value was shown for the four microform strata groups in terms of macrofossils. The results are displayed in Figure 12. The deviance value was relative to the shallowest distance value, since this is the youngest macrofossil measurement and is most closely related to the size and type of the microforms.

$$\text{Deviance value} = A \log(\text{depth}) - B \quad (\text{eq. 9})$$

Where the deviance value is based on the absolute distance of the plant species and the depth is measured in cm. A and B are the parameters calculated using the nls() function in R (Team, 2014). Parameter A is the value that is most important for the gradient of the deviance, since this value regulates the smoothing of the deviance value over depth. The higher the value of A, the longer it takes before the deviance value reaches an asymptote. Parameter B is the starting value at zero depth. For the large hollows, parameter A and B are significant (Table 12 - Table 15, in appendix).

3.5.3. Statistics

The K_{sat} data, was tested for Homogeneity of variances via the Levene's test on the microform strata and depth combinations. A threshold of ($P > 0.05$) was used. And the K_{sat} data was tested for Normality on the microform strata and depth combinations via a

Shapiro-Wilk test with a threshold of ($P > 0.05$). A log transformation of the K_{sat} data resulted in the best results in terms of homogeneity and normality, compared to the non-transformed K_{sat} data and the Tukey transformed K_{sat} data.

For research questions 1a and 1b, the non-transformed K_{sat} data was fitted against depth via a nonlinear (weighted) least-squares algorithm and the 5% and 95% confidence band of that fit was produced, to determine whether the functions are significantly different (Team, 2014). The 5% and 95% confidence bands are created with a Monte Carlo simulation with 100,000 simulations (predictNLS function in R).

To determine which environmental variable influences the K_{sat} (dependent variable), a linear mixed-effects model is created in R. The mixed effect model was chosen since there is a need for fixed effects and random effects. The K_{sat} is the dependent variable and transformed into $\log_{10}(K_{sat})$, since the Normality and the Homogeneity test show better results. The fixed effects are the covariates: the von Post scale, water content, bulk density (all scaled between 0-100), all these variables are continuing variables and do not require to be seen as different groups. More fixed effects as factor are: the depth kept in cm (0-150), the type of microform (hollow/hummock) and the relative size (big/small), for these variables a distinction can be made between different groups and should be treated as factors. The six different sites were chosen to be the random effect in the models, this to adjust for the likelihood that measurements close to each other (with the same site number) could be more similar. The depth was set as repeated measure the subjects type of microform, microform size and site number. The total dataset had 66 samples, there was no selection on the K_{sat} data. A maximum of nine independent variables would be used to explain the K_{sat} . To analyse the variation in K_{sat} that a single variable could explain, anova type 2 was chosen accompanied with the significance level. The AIC was used to choose the best model (Burnham & Anderson, 2003) and when the level of ($P < 0.05$) was not exceeded, a variable was included as a determining variable for the K_{sat} . The models were created based on parameters that proved to influence the K_{sat} in literature (e.g. (Morris *et al.*, 2015)). Every time a new model was created the new parameter was evaluated and accepted or discarded. Another option could be a AIC stepwise algorithm, however a more research question driven search was preferred.

Canoco (v. 5.04) was used to gain insight in the relationship between macrofossil composition and hydrophysical variables. A principal components analysis (PCA) was performed. This method is commonly used in studies of modern ecology and vegetational succession (Lepš & Šmilauer, 2003). With this type of analysis, a two-dimensional plot is created, showing variance with the dataset on a series of axis. Taxa that frequently co-occur are plotted together, while those that rarely co-occur are furthest apart. The greatest variation is shown on the first axis, whereas the second axis explains less variation and so on. A redundancy analysis (RDA) is done to determine which environmental variables were significantly able to explain the variation found in the macrofossil data. A forward selection of explanatory variables was used for this purpose.

The PCA and RDA analyses are done on the same dataset (90 samples, distributed in 21 plant classes, for 11 environmental variables). This analysis summarizes the variation in species composition using the data in 'Species' table and interprets this summary with the help of environmental variables. The input for the PCA and RDA analyses were the environmental variables: depth of the sample (in cm below the water level), K_{sat} (in m/d), von Post scale (1-9), water content of the sample (%), bulk density (g/m^3), minimal size in (m), maximal microforms size (m), area of the microform (m^2), perimeter of the microform (m), estimated size in the field (m), all scaled between 0-1 in the software program. The type of pattern (maze, string or dotted) was included as factor. Also, the count of the macrofossils (original whole numbers ranging from 0-100, now 0-1). This to create an equal distribution between the different variables.

To gain insight into the pedological memory of the microforms, the same procedure was used as for the gradient of K_{sat} over depth (question 1). The input was the deviance value for each of the types of microforms (big/small and hummock/hollow).

To research whether a microform has a strong pedological memory, a cluster dendrogram was made and p-values are calculated for hierarchical clustering via multiscale bootstrap resampling. The clustering method for this analysis is 'ward', since it uses the nearest neighbour. In the analysis, the Euclidean distance is used as method and 10000 was used as the number of bootstrap replications. The individual clusters were selected based on a threshold value of 0.95 for p-values. The cluster dendrogram was made using the pvclust package in R.

4. Results

4.1. K_{sat} gradient over depth and differences between microforms

1a) Is there a vertical K_{sat} gradient over depth?

On the combined dataset of all microforms and all the relative sizes, a significant decline of the K_{sat} over depth was found (Table 2). The saturated horizontal hydraulic conductivity can reach up to 25 m/day in the upper part of the peat profile, whereas it decreases rapidly to around 1 m/d at a depth of 50 cm. This value stays more or less constant until a depth of 150 cm.

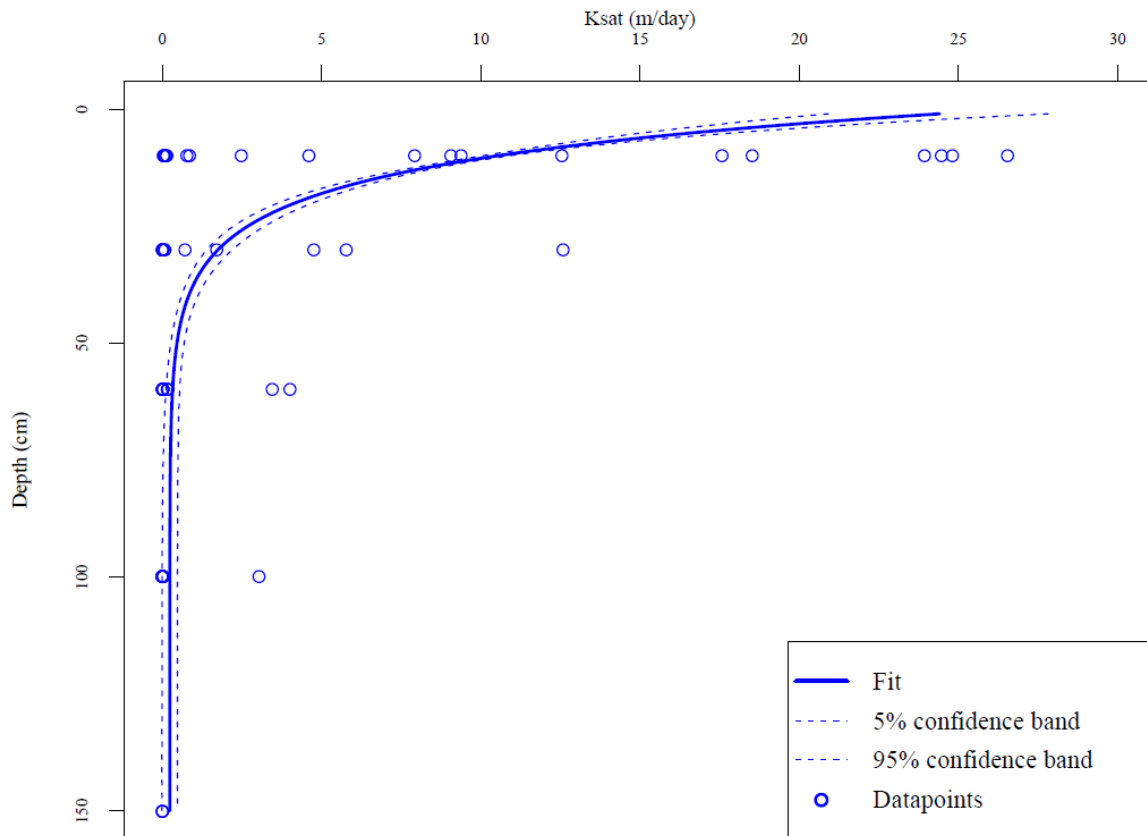


Figure 6. The blue line is the fit function on all the K_{sat} data. The plotted function is eq.7. For the values of the parameters, see Table 2. The dashed lines are the 5% confidence band and the 95% confidence band of the Monte Carlo fit. $n=66$ samples.

The result of the fit of the equation 7 on the K_{sat} data is shown in (Figure 6 and Table 2). Parameter A determines the gradient slightly. Whereas parameter B is important for the gradient of the K_{sat} against the depth (sensitivity analysis, not shown here). Parameter C is the start value of the K_{sat} at depth zero. To answer the research question, parameter B is most important (sensitivity analysis, not shown here).

Parameter A is significant ($P < 0.05$) (Table 2). The P-value for parameter B is also significant, with a P-value of 0.00948. Parameter C is not significant and could better not have been included. Parameter C is the start value of the K_{sat} (theoretically the ground water level). Hereby parameter B confirms that there is a gradient in the K_{sat} with depth. The results show that there is a gradient of the K_{sat} over depth.

Table 2. Parameter values all sites, standard errors, t value and P value. $n=66$.

Based on all the data				
Parameter	Estimate	Std. Error	t value	Pr(> t)
A	26.59	2.482	10.71	0.008602
B	0.0953	0.009348	10.20	0.009480
C	0.2316	0.1482	1.563	0.2584

1b) Is there a difference in K_{sat} between hummocks and hollows?

The hummocks have lower values than the hollow for all depths on average. The K_{sat} for the hollows is higher than 30 m/day at a few centimeters beneath the water level, after which it rapidly declines to low values at a depth of 60 cm below the ground water level (Figure 7). For the hummocks, the highest horizontal hydraulic conductivity has a maximum value of around 15 m/day and decreases to low values at a depth of 15 cm.

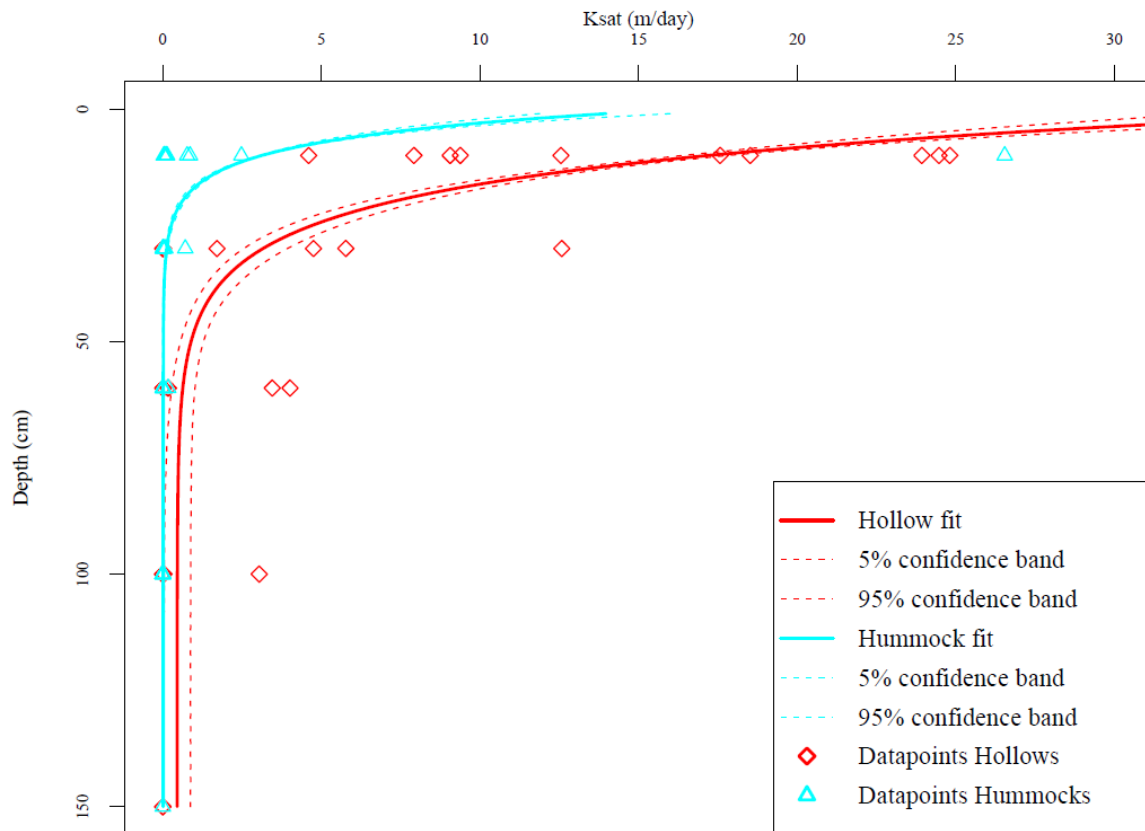


Figure 7. The cyan and red lines are the fit functions for the hollow and hummock K_{sat} data. The plotted function is eq. 7. For the values of the parameters, see Table 3. The dashed lines are the 5% confidence band and the 95% confidence band of the Monte Carlo fit. $n=34$ hollows samples and $n= 32$ hummocks samples.

Parameter A is higher for the hollow compared to the fit for all the data and the hummock (Table 3), confirming that hollows are more conductive at low depth compared to hummocks. A lower value for B for the hollows compared to the hummocks also results in higher values at lower depth and a slower decrease of the gradient for K_{sat} over depth. A higher value for parameter C results in a higher start K_{sat} value for the hollows compared to the hummock in neither of the microforms this parameter could have been included, since it is not significant.

The fitted lines in Figure 7 are based on (eq.7) and parameters A, B and C (Table 3).

Table 3. Parameter values Hollows (n=34) and Hummocks (n=32), standard errors, t value and P value.

Parameter	Hollows				Hummocks			
	Estimate	Std. Error	t value	Pr(> t)	Estimate	Std. Error	t value	Pr(> t)
A	41.60	3.791	10.97	0.008203	16.50	1.636	10.09	0.009687
B	0.09113	0.009072	10.05	0.009765	0.1672	0.01005	16.64	0.003592
C	0.4558	0.2563	1.778	0.2174	0.01451	0.01109	1.308	0.3209

4.2. K_{sat} in relation to other (environmental) variables and the predictive power of environmental variables on microfossil composition

2a) How are K_{sat} values related to other environmental variables?

The K_{sat} was log transformed to account for the general shape of the K_{sat} over depth, see results question 1. Furthermore, the untransformed K_{sat} data displayed larger departures from both homoscedasticity and linearity, both were largely remedied by this transformation. The transformation also ensured that model predictions would always be strictly positive (negative values of K_{sat} are physically meaningless).

Table 4. Overview of some of the model created. For all the models site was the random factor and depth was the repeated measure. hol/hum is a dummy variable for hummock/hollow, big/small is a dummy variable for the relative size of the microform, depth is depth of the measurements (cm), vPost is the von Post scale, Bd is the bulk density in (g/cm³) and wc is the water content [%], n=66 samples for all the variables.

# of the model	Variables used	AIC	Δ AIC
14 (reference model)	$\log(K_{sat}) = \text{hol/hum} \times \text{big/small} \times \text{depth}$	271	0
20	$\log(K_{sat}) = \text{hol/hum} + \text{big/small} + \text{depth} + \text{vPost}$	280	+9
21	$\log(K_{sat}) = \text{hol/hum} + \text{big/small} + \text{depth} + \text{vPost} + \text{Bd}$	287	+16
22	$\log(K_{sat}) = \text{hol/hum} + \text{big/small} + \text{depth} + \text{vPost} + \text{Bd} + \text{wc}$	294	+23
23	$\log(K_{sat}) = \text{hol/hum} \times \text{big/small} \times \text{depth} + \text{vPost}$	263	-8
24	$\log(K_{sat}) = \text{hol/hum} \times \text{big/small} \times \text{depth} \times \text{vPost}$	333	+62

$$\log(K_{sat}) = -2.27 \text{ hol/hum} * 0.05 \text{ big/small} * (-3.13/-2.78/-7.09/-7.41) \text{ depth} * 0.0542 \text{ vPost} + 3.67 \quad (\text{eq. 10})$$

Where K_{sat} is the hydraulic conductivity (m/day), depth is the measured depth (cm), hol/hum is a dummy variable for the type of microform, big/small is a dummy variable for the size of the microform and the von Post scale [0-10] (the significant parameters are in bold). The bulk density and the water content do not have a predictive value for the K_{sat} .

Table 5. Summary of the fixed effects in the linear mixed effects model fitted to the log₁₀-Transformed K_{sat} data (see also equation 10)

Variable	Coefficient	Standard error	t-value	Pr (>Chisq)
(intercept)	3.67235	0.78464	4.680	
hol/hum (hummock)	-2.26636	1.02371	-2.214	9.309e-05 ***
big/small (small)	0.05710	0.97013	0.059	0.1501
depth (30cm)	-3.12852	1.03959	-3.009	2.346e-07 ***
depth (60cm)	-2.77634	1.13135	-2.454	2.346e-07 ***
depth (100cm)	-7.09371	1.61006	-4.406	2.346e-07 ***
depth (150cm)	-7.41205	2.57233	-2.881	2.346e-07 ***
von Post	-0.05421	0.01115	-4.860	1.175e-06 ***

The linear mixed effects model predicts that the log-transformed K_{sat} decreases with increasing depth. Furthermore, the model predicts that K_{sat} is lower beneath hummocks than hollows and the log-transformed K_{sat} decreases with increasing von Post values (Table 5). The model performs accurate in terms of R^2 however the RMSE could have been lower, but this is a relative measure (Figure 8).

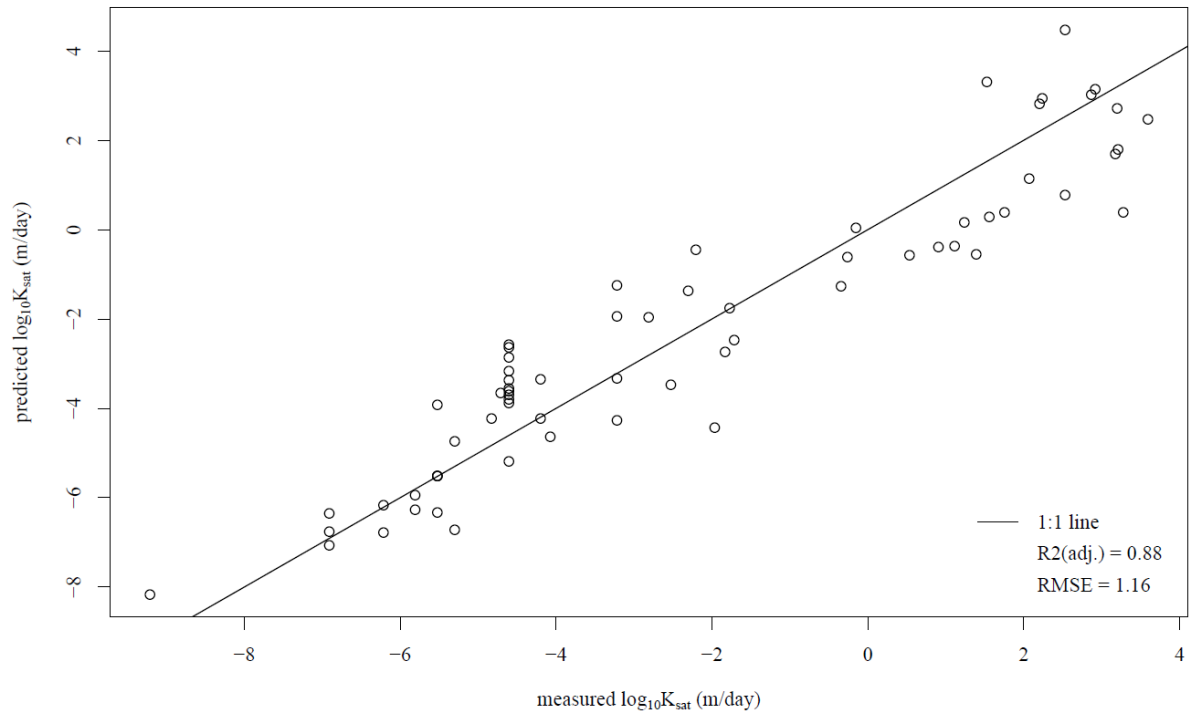


Figure 8. Performance of the linear mixed effects model (eq. 10), showing its predicted values of peat saturated hydraulic conductivity against the measured values used to generate the model.

2b) Relation between peat botanical composition and hydrophysical characteristics

To determine whether the macrofossil data can be explained by the environmental variables, this analysis summarizes the variation in species composition using the species data and interprets this summary with the help of environmental variables.

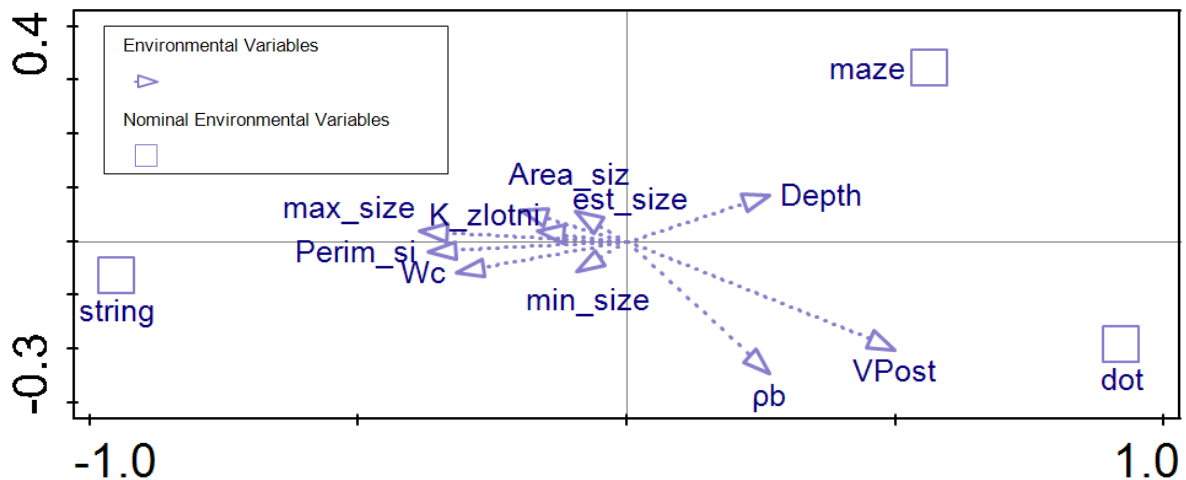


Figure 9. Ordination diagram (PCA) of the first two ordination axes, showing the environmental variables possibly explaining the variation in vegetation composition (eigenvalue Axis 1=0.209, eigenvalue Axis 2=0.120). K_{sat} is the K_{sat} , Wc is the water content, pb is the bulk density, $VPost$ is the von Post, $Depth$ is the depth of the sample, $string$, $maze$ and dot are the type of pattern, max_size is the maximal size of the microform, min_size is the minimal size of the microform, est_size is the estimated size of the microform in the field, $Area_siz$ is the area of the microform and $Perim_si$ is the perimeter of the microform.

The K_{sat} is negatively related to the depth of the samples, this result is in line with the decrease of the K_{sat} over depth found in the previous research question (correlations coefficient = -0.389 ($p=0.000$)). The K_{sat} is negatively related to the von Post (correlations coefficient = -0.430 ($p=0.000$)). The bulk density does not have a negative relationship with the K_{sat} (correlations coefficient = -0.134 ($p=0.194$)). The K_{sat} is positively linked to the water content (correlations coefficient = -0.126 ($p=0.225$)). Furthermore, the maximal and perimeter size of microforms is positively correlated with the K_{sat} (correlations coefficient = 0.007), ($p=0.945$), (correlations coefficient = 0.064 ($p=0.536$)). The area size of the microforms is positively correlated with the K_{sat} (correlations coefficient = 0.231 ($p=0.024$)). String patterns are positively correlated to the K_{sat} . All the environmental variables together can explain 22.4% (Adjusted variation explained 11.1%) of the species composition, see PCA and RDA analyses in appendix for the summary of the PCA.

To test which environmental variables have a significant effect on the plant species, a RDA was performed. The RDA showed via stepwise forward regression that the von Post, water content, pattern types and the K_{sat} explained the species composition for a total of 15.7% (11.9% adjusted variation explained). The von Post was most important in explaining species composition (Table 6).

Table 6. Forward selection results of the RDA:

Name	Explains %	Contribution %	pseudo-F	P	P(adj)
Von Post	6.8	30.4	6.8	0.001	0.013
Water content	4.8	21.5	5.0	0.001	0.013
Pattern type	2.5	11.0	2.6	0.001	0.013
K_{sat}	1.6	7.1	1.7	0.089	1.

The K_{sat} does not significantly contribute to the variation in macrofossil composition (Table 6), however was included since this report focuses on the K_{sat} . Figure 10 shows only the variables which are significantly contributing to variation in macrofossil composition, calculated by the RDA. These four variables have an explained variation of 16.2% (adjusted explained variation of 11.5%) on the species composition. The von Post is negatively related to the K_{sat} (correlations coefficient = -0.430 ($p=0.00$)). The water content is positively related to the K_{sat} (correlations coefficient = -0.104 ($p=0.40$)), whereas the string patterns have a higher K_{sat} and water content compared to the dot - and maze patterns. The von Post scale is not related to the water content (correlations coefficient = -0.025 ($p=0.810$)) (Figure 9, Figure 10).

All the Sphagnum sections are located in the left and are therefore somewhat similar in response to the environmental variables (Figure 10). The Sphagnum sections Acutifolia, Palustre and Cuspidata are correlated to the total Sphagna group (correlations coefficient = .678 (p= 0.000)), (correlations coefficient = .325 (p= 0.001)), (correlations coefficient = .752 (p= 0.000)), but not with the other sections. The *Carex limosa* and the *Carex sp.* group are correlated with each other (correlations coefficient = .809 (p= 0.000)), the *Carex limosa* is a sub specie of the *Carex sp.* group and it is expected that the groups are related. *Scheuchzeria palustris* is closely correlated with the *Drepanocladus sp.* and the *Rhynchospora alba* (correlations coefficient = .448 (p= 0.000)), (correlations coefficient = .434 (p= 0.000)). Furthermore, the *Aulacomnium Palustre* is closely correlated with the Brown mosses group (correlations coefficient = .389 (p= 0.000)). Ericaceous bark is also closely related to the Ericaceous roots (correlations coefficient = .435 (p= 0.000)). Roots are likely to penetrate though several tens of cms of peat, therefore such a strong correlation is remarkable since tens of cms can represent a long time in which the vegetation can change.

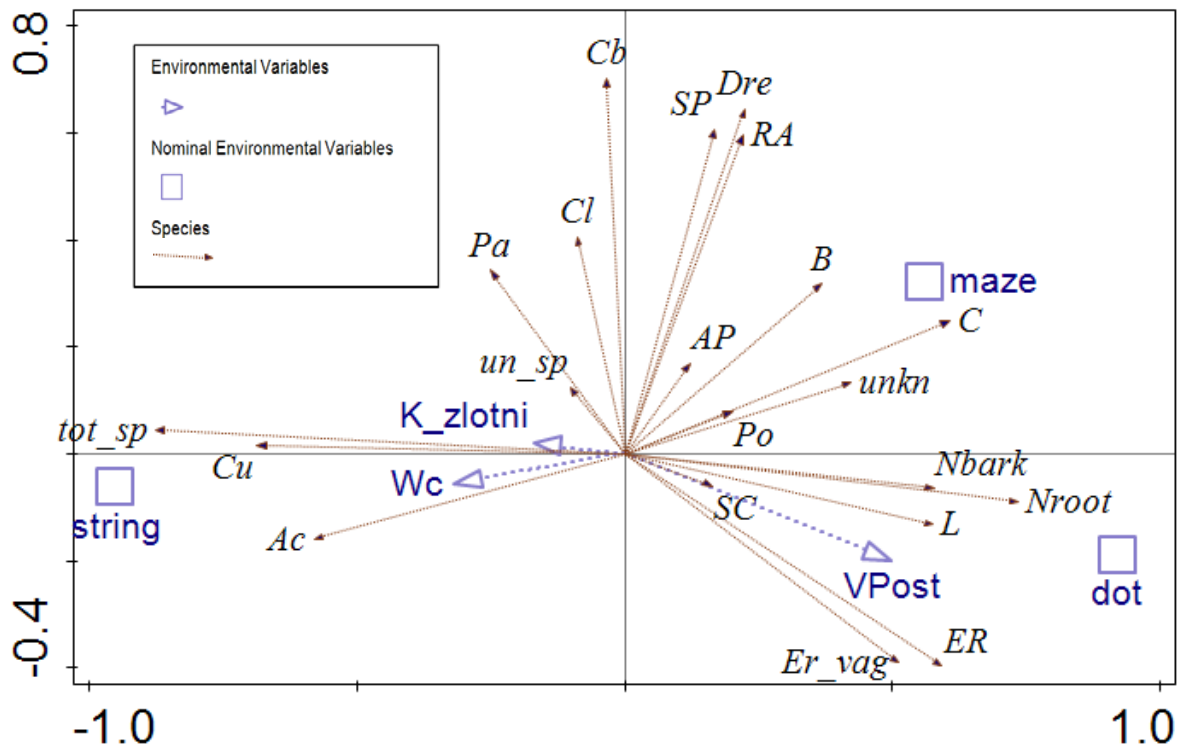


Figure 10. Ordination diagram (PCA) of the first two ordination axes, showing the environmental variables responsible for the variation in vegetation composition and the vegetation groups (eigenvalue Axis 1=0.209, eigenvalue Axis 2=0.120). K_zlotni is the K_{sat}, Wc is the water content, VPost is the vonPost, string, maze and dot are the type of pattern. Ac= Sph. Acutifolia, Pa= Sph. Palustre, Cu = Sph. Cuspidata, un_sp=unidentified Sph., tot_sp= Total Sph., Po = *Polytrichum sp.*, B=brown mosses, Nroot=Ericaceous roots, Nbark=Ericaceous bark, L = trees and shrubs, Er_vag= *Eriophorum vag.*, C=*Cyperaceae sp.*, ER=*Eriophorum sp.*, Cl=*Carex limosa*, Cb=*Carex sp.*, Dre=*Drepanocladus sp.*, RA=*Rhynchospora alba*, Sp=*Scheuchzeria palustris*, A.P.=*Aulacomnium palustre*, S.C.=*Scirpus cespitosus*, unkn=unknown fragments.

The total Sphagnum group has a positive relationship with the K_{sat} (correlations coefficient = .187 (p= 0.069)), although the K_{sat} has a negative relationship with the Ericaceous root group (correlations coefficient = -.234 (p= 0.023)) which is the only macrofossil group that has a significant relationship with the K_{sat}. The Sphagnum Cuspidata and Sphagnum Acutifolia sections are related to the string pattern. Whereas the Brown mosses and the *Cyperaceae sp.* are more dominant in the maze patterns. And the dotted patterns have the largest quantities of Lignin's (trees and shrubs) and Ericaceous root, - bark fragments. This type of vegetation is mostly seen in more drier environments. The water content has the strongest positive relationship with the total Sphagnum group (correlations coefficient = .307 (p= 0.003)). *Aulacomnium palustre* has the strongest negative relationship with the water content (correlations coefficient = -.461 (p= 0.000)). The von Post has the strongest positive relationship with the *Eriophorum sp.* (correlations coefficient = .457 (p= 0.000)). And the von Post has a positive relationship with the lignin's (trees and shrubs) (correlations coefficient = .381 (p= 0.000)). The Sphagnum Cuspidata section has the strongest negative relationship with the von Post (correlations coefficient = -.480 (p= 0.000)).

2c) Do the type and surface area of microform patterns influence K_{sat} ?

Since height and vegetation differences for hummock and hollow are visible in the field or via aerial images/remote sensing, it would give insight if there is a relationship between physical properties of the soil and microform type. The best model to predict the K_{sat} on 10 cm depth below the groundwater level will only need the information of the type of microform (Table 7, model 40, P-values not shown). Model 46 gives the most insight, since the minimal size of the microform and the area size of the microform give significant information about the K_{sat} (Table 8). The bulk density and the water content do not have a predictive value for the K_{sat} .

Table 7. Overview of some of the models tested, for all the models site was the random factor. hol/hum is a dummy variable for hollow/hummock, big/small is a dummy variable for big/small microform, Min is the minimal size, Max is the maximal size, Area is the size of the area, Est is the estimated size, Perim is the perimeter of the microform, Vpost is the vonPost, Wc is the water content, Bd is the bulkdensity, n= 21 samples, for all the variables.

# of the model	Variables used	AIC	Δ AIC
40 (reference model)	$\log(K_{sat10}) = \text{hol/hum} \times \text{big/small}$	83	0
41	$\log(K_{sat10}) = \text{hol/hum} + \text{big/small}$	82	-1
42	$\log(K_{sat10}) = \text{hol/hum} \times \text{big/small} + \text{Min} + \text{Max} + \text{Area} + \text{Perim} + \text{Est}$	115	+32
43	$\log(K_{sat10}) = \text{hol/hum} \times \text{big/small} + \text{Min} + \text{Max} + \text{Area} + \text{Perim} + \text{Est} + \text{VPost} + \text{Wc} + \text{Bd}$	134	+51
46	$\log(K_{sat10}) = \text{hol/hum} \times \text{big/small} \times \text{Pattern type} + \text{Min} + \text{Max} + \text{Area}$	102	+19
45	$\log(K_{sat10}) = \text{hol/hum} \times \text{big/small} + \text{Min} + \text{Max} + \text{Area}$	103	+20

The most suitable formula for this research question (number 46):

$$\log(K_{sat10}) = -1.95 \text{ hol/hum} - 0.111 \text{ Min} + 0.140 \text{ Area} + 2.13 + 0.727 \text{ big/small} + (0.570/-0.370) \text{ Pattern type} - 0.0263 \text{ Max} - 1.13 (\text{hol/hum} * \text{big/small}) \quad (\text{eq. 11})$$

Where K_{sat10} is the hydraulic conductivity at 10 cm depth (m/day), hol/hum is a dummy variable for the type of microform, Min is the minimal length of the microform (m), Area is the area of the microform (m²), big/small is a dummy variable for the size of the microform, Pattern type is a dummy variable for the microform patterns (string, dotted and maze), Max is the maximal length of the microform (m) (the significant parameters are in bold).

Table 8. Summary of the fixed effects in the linear mixed effects model fitted to the log₁₀-Transformed K_{sat10} data. Hol/hum is a dummy variable for hollow/hummock, big/small is a dummy variable for big/small microform, Min is the minimal size, Max is the maximal size, Area is the size of the area. Pattern type are the type of pattern.

Variable	Coefficient	Standard error	t-value	Pr (>Chisq)
(intercept)	2.12910	1.39982	1.521	
Hol/hum (hummock)	-1.95393	1.56239	-1.251	0.005809 **
Big/small (k)	0.72695	1.20215	0.605	0.859630
Pattern type (2)	0.57037	1.45249	0.393	0.806475
Pattern type (3)	-0.37020	1.32057	-0.280	0.806475
Min	-0.11129	0.06610	-1.684	0.092252 .
Max	-0.02634	0.02045	-1.288	0.197816
Area	0.13973	0.07276	1.920	0.054803 .
Hol/hum x big/small	-1.13047	1.63769	-0.690	0.490015

The linear mixed effects model predicts that the log-transformed K_{sat} in the 10 cm below the groundwater layer is mostly influenced by the type of microform (hollow or hummock) which is negatively for hummocks. And the log-transformed K_{sat} is negatively influenced by the minimal size and positively by the area size of the microform. Although the best model (Table 7) only depended on the dummy variable for the type of microform. Model 46 performs accurate in terms of R² however the RMSE could have been lower, but this is a relative measure (Figure 11).

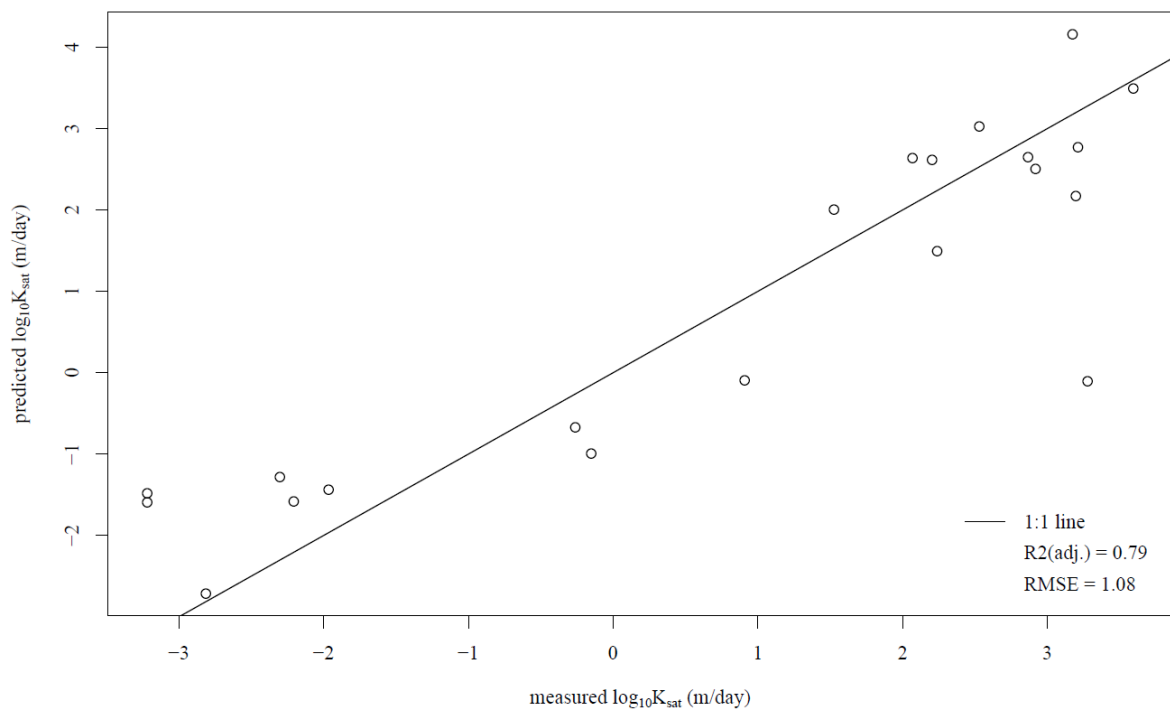


Figure 11. Performance of the linear mixed effects model (equation 11), showing its predicted values of peat saturated hydraulic conductivity against the measured values used to generate the model.

4.3. Pedological memory in peatland microforms

3a) Do large microform have higher similarity than smaller microforms, in terms of macrofossils?

The distance value per microform and size was calculated, based on differences in macrofossils counts (Table 11, in appendix). The deviance value was created based on eq. 9. Not all the microform type and - size combinations had significant results for parameter A and B (Table 12 - Table 15, in Appendix). For the large hummocks, parameter A and B are not significant (Table 13, in Appendix). For the small hollows, parameter A and B are significant (Table 14, in Appendix). For the small hummocks, parameter A is significant and B is not significant (Table 15, in Appendix).

Although the parameters for the large hummocks are not significant in (Table 13, in Appendix), it is clearly visible that it is likely that the larger microforms have a lower deviance value (Figure 12). Confirming the fact that larger microforms (hummocks and hollows) are more persistent over depth and thereby more resilient towards external factors.

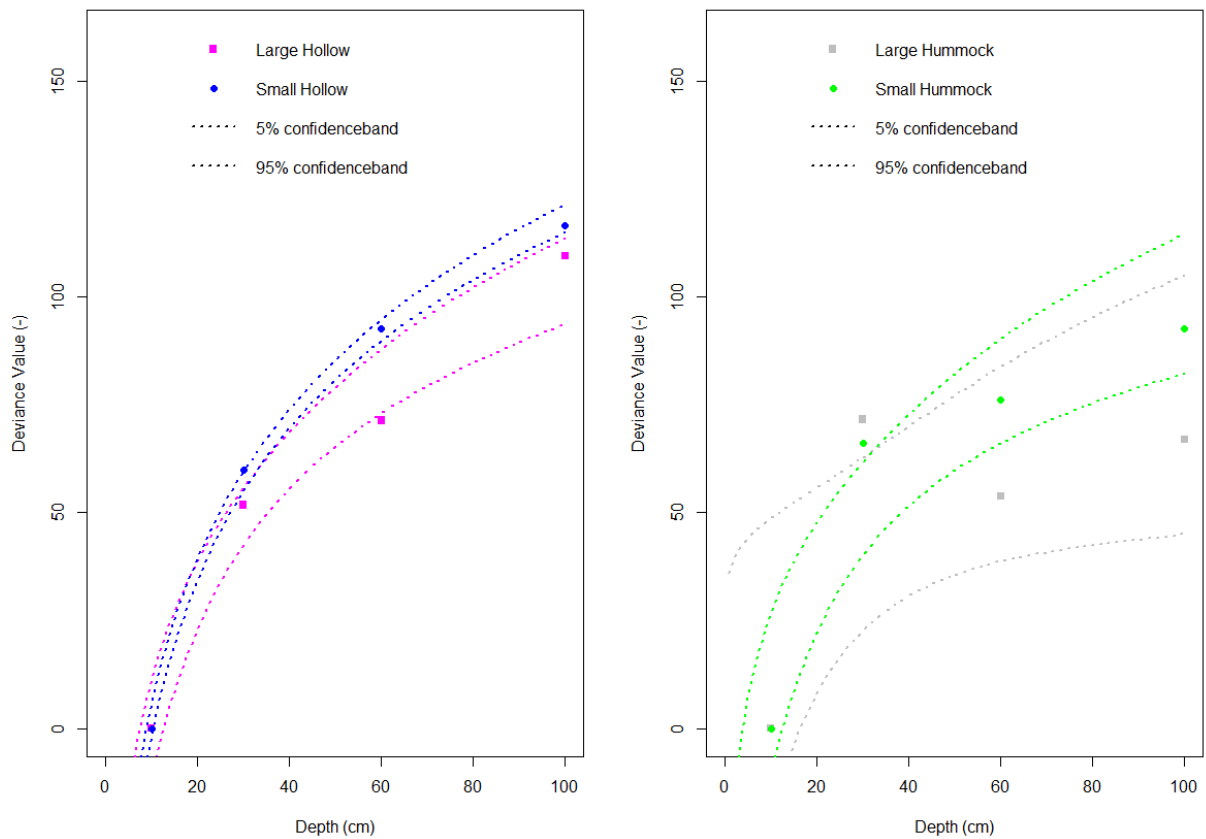


Figure 12. Deviance value of the plant macrofossils over depth below the groundwater level. The squares and dots are the deviance values for the microforms. The dashed lines are the 95% and the 5% confidence band per microform class.

The four microform classes differ in their peat profile in terms of macrofossils, degree of decomposition, water content and bulk density (Figure 13 - Figure 16). Taxa indicative of surface wetness (water level close to the surface) are more abundant in the large and small hollow class, compared to the large and small hummock class. For example, the hollow classes have a larger number of proportion of *Sphagnum Cuspidata* section compared to the hummock classes. Whereas this is reversed for the *Sphagnum Acutifolia* section, also the hummock classes have larger amounts of Ericaceous dwarf shrubs. *Aulacomnium Palustre* is visible in a hummock sample, however this species tolerates a lot of moisture regimes, but is more commonly seen in depressions in the landscape, places where moisture occurs (Larsen, 2013).

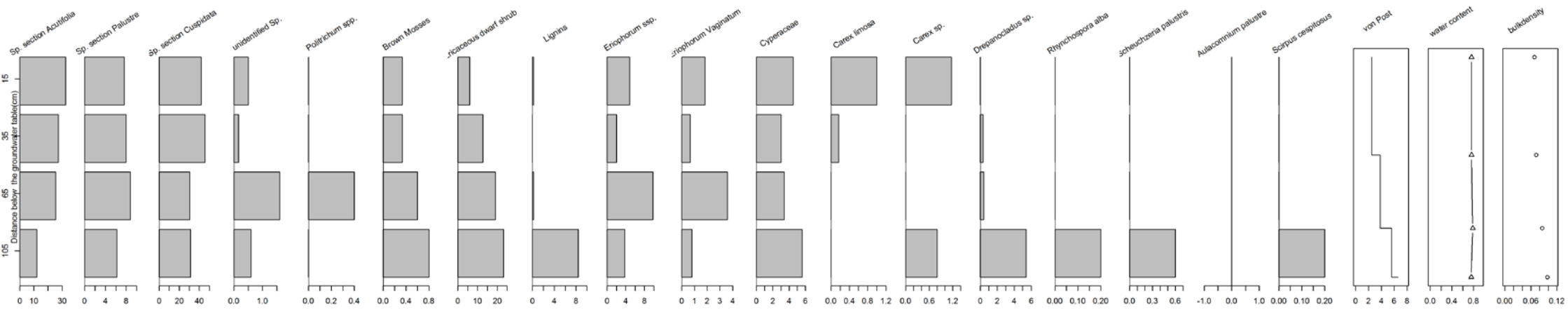


Figure 13. The macrofossil analysis (%), Von Post humification degree (1-9), water content (fraction) and dry bulk density (g/cm^3) data averaged for the large hollows

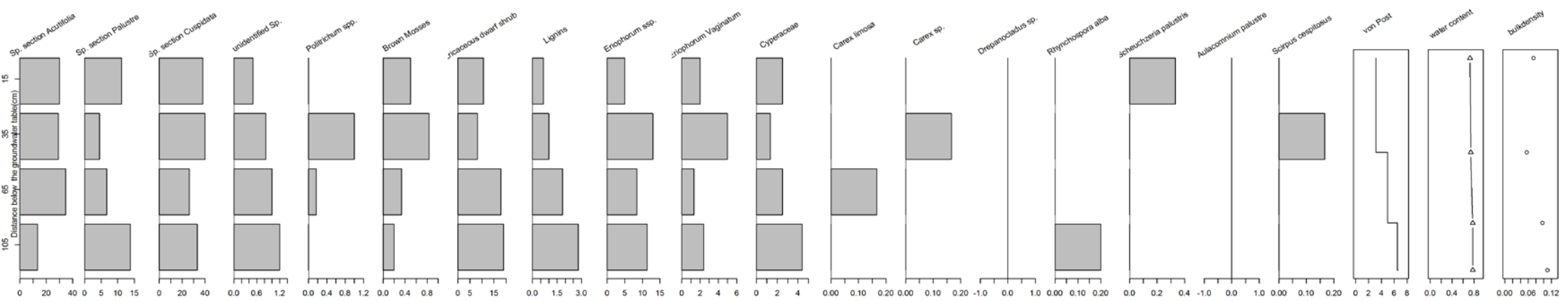


Figure 14. The macrofossil analysis (%), Von Post humification degree (1-9), water content (fraction) and dry bulk density (g/cm^3) data averaged for the small hollows

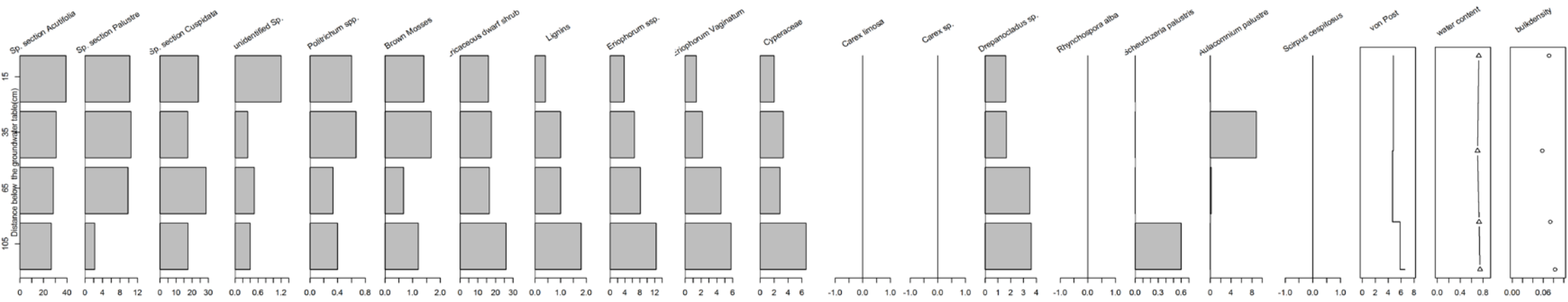


Figure 15. The macrofossil analysis (%), Von Post humification degree (1-9), water content (fraction) and dry bulk density (g/cm^3) data averaged for the large hummocks

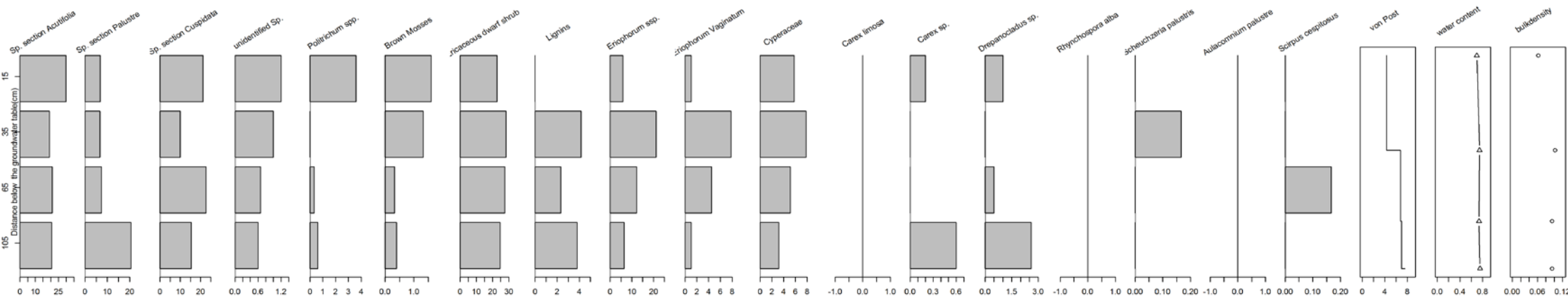


Figure 16. The macrofossil analysis (%), Von Post humification degree (1-9), water content (fraction) and dry bulk density (g/cm^3) data averaged for the small hummocks

3b) Pedological memory per site

The focus for this sub research question will be on the individual macrofossils found in a core. Peat cores strongly differentiated over depth (Figure 17)(Table 10, in appendix). None of the cores remains in the same cluster over the whole depth. This proves that plant composition changes over depth (time). Some of the cores do have most depths in the same cluster e.g. 3gu in cluster 1. When this is the case, the pedological memory is large. On the other hand, 1gu occurs in cluster 4, 7, 5 and 13. This site would have a low pedological memory.

Whether a site remained a hollow or a hummock, indicating it has large persistence, is not directly visible. Site 3gu contains on all depths measured only low amounts of the *Sphagnum Acutifolia* section and none or low amounts of the *Sphagnum Palustre* section. At a depth of 30 cm, Site 3gu has no remains of the *Sphagnum Cuspidata* section, whereas the other samples in cluster 1 do have remains in this section, ranging from 16% until 31% and $\leq 1\%$ in the *Polytrichum* section. Values for the Ericaceous root from 12% until 34% and for Ericaceous bark 1% until 6%. Remarkably, core 3gu from 30 cm depth has 53% remains of *Aulacomnium Palustre*, whereas the other samples has 1 as highest. 3gu, at 30 cm, is therefore probably excluded from the cluster. Based on the values for the *Sphagna* sections, site 3gu from 60 cm until 150cm is likely to have been a hollow.

Site 1gu begins with 44% of the *Sphagna* section *Acutifolia* at 10 cm at has the lowest value of 32% at 100 cm. The *Sphagna Cuspidata* section changes from 31% at 10 cm depth to 24% at 30 cm, has a value of 37% at 60 cm and ends with 14% at 100 cm depth, whereas the Ericaceous roots show an opposite development. This variation within the profile causes the different depths to fall within different clusters, indicating a low pedological memory, based on the number of clusters the site is in (Figure 17). Only at a depth of 100 cm the difference between the *Sphagna* in the *Acutifolia* and the *Sphagna* in the *Cuspidata* section is that large that it could have been a hummock.

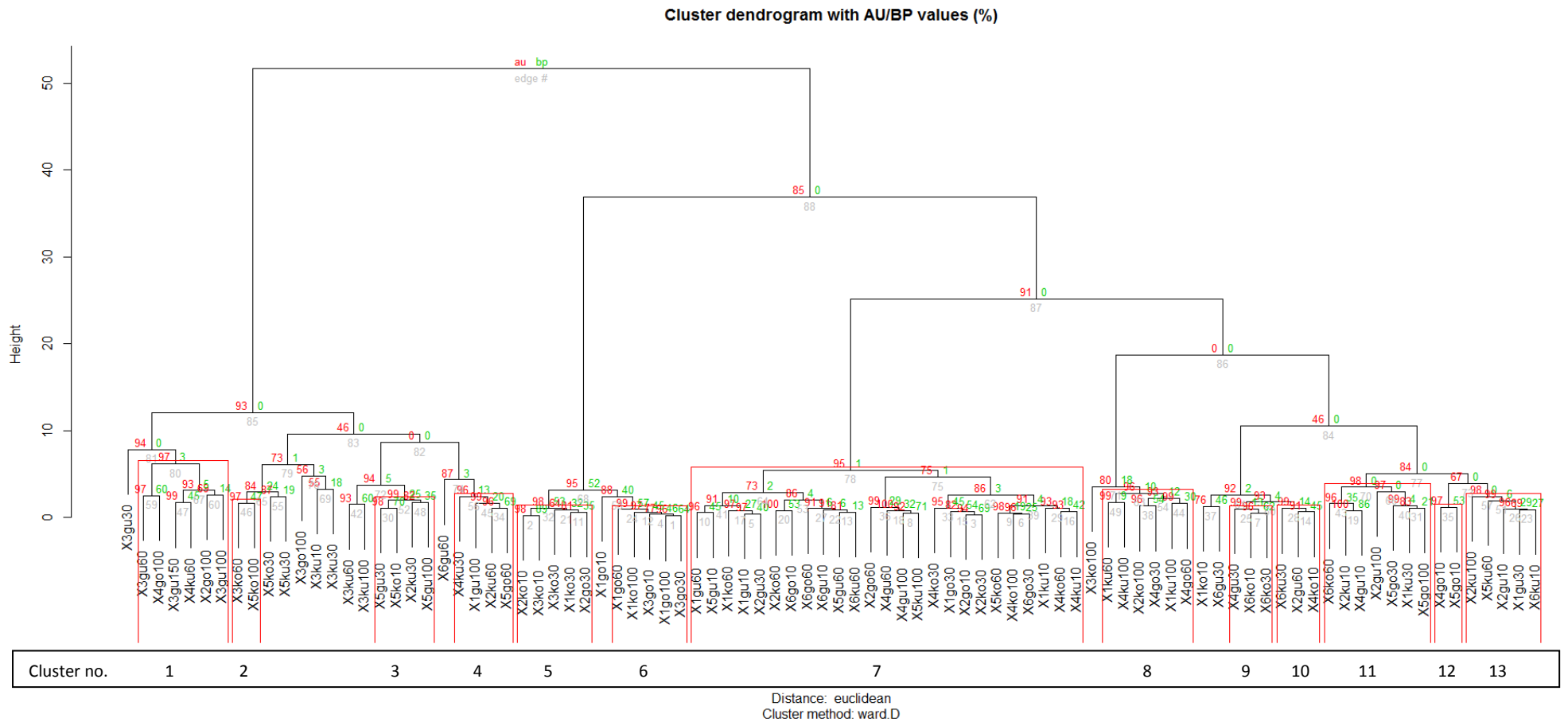


Figure 17. Cluster dendrogram of the plant macrofossil data. The number refers to the site, the g for large microforms, the k for small microforms, whereas the o refers to a hollow and the u for a hummock. The remaining digits refers to sample depth in cm. Euclidian distance and 'Ward.D' cluster method were used to construct the dendrogram. Two types of P-values are shown: au (Approximately Unbiased - in red) P-value and (Bootstrap Probability - green) value, clusters are numbered from left to right (n=13)

5. Discussion

5.1. K_{sat} gradient over depth and differences between microforms

The results of this study clearly show a gradient over depth and between different microforms for the K_{sat} . In contrast with (Holden & Burt, 2003) which uses the response time chart of (Brand & Premchitt, 1982) to see whether there is a decrease of the K_{sat} over depth, this study shows that there is a significant decline in K_{sat} for the first 150 cm below the ground water level (Table 2). This finding is in agreement with existing literature (Branham & Strack, 2014; Grover & Baldock, 2013; Ingram, 1983; Morris *et al.*, 2015; Price *et al.*, 2003; Whittington *et al.*, 2007).

Morris *et al.* (2015) found a lower value of the hollows and a higher value for the hummocks in K_{sat} for a bog peatland in southern Sweden which is in disagreement with this study. However, this study shows that there is a significant difference between the microform types. In Branham and Strack (2014) is stated that Ivanov (1975) suggested that K_{sat} is at least an order of magnitude greater in wet (hollow) microforms compared with dry (hummock) microforms. This is confirmed for a part of the transect in Figure 7. However, it is questionable if this will hold for greater depth or for the upper part of the profile. Whether the differences may be important if those K_{sat} values are low at greater depth is also questionable (Baird *et al.*, 2016). However, proving that K_{sat} is lower in hummocks than hollows up to a depth of about 75cm below groundwater level, our results support the pillar theory (Belyea & Baird, 2006; Moore, 1977). Without a difference in K_{sat} values between microform types it would be hard to use the K_{sat} value as a measure to predict a pillar. Difference in K_{sat} for different microforms could prove that microform vegetation has self-regulation abilities in terms of wetness, which result in microform patterns throughout the peatland.

These findings are in contrast with (Branham & Strack, 2014) which states no difference between hummock and hollows in terms of K_{sat} over depth, measured in-situ. The given reason is a difference in pore size distribution between hummock and hollows over depth. This study did not take the pore size into account.

5.2. K_{sat} in relation to other (environmental) variables?

2a) How are K_{sat} values related to other environmental variables and how can environmental variables explain variation in macrofossils?

The von Post, type of microform (hummock or hollow) and the depth can be used to predict the K_{sat} (Table 5). The von Post scale is negatively correlated with the K_{sat} . The deeper the sample the higher the von Post scale, in accordance with (Päivänen, 1973). Due to different forming processes of the peat, this relationship could be different when the bottom of the peat layer would be reached. For the first 150cm below the ground water level, the sample depth is more important for the K_{sat} (eq. 10).

In contrast with (Branham & Strack, 2014) the bulk density does not add much explaining value in the models for the K_{sat} value. A possible explanation could be that in (Branham & Strack, 2014) K_{sat} was measured in the lab, whereas the K_{sat} in this research was measured in-situ. Branham and Strack (2014) did find a relationship with the von Post, microform type and depth for the K_{sat} which is in agreement with this research (eq. 10).

The von Post, water content and type of pattern (string pattern) are the only environmental variables that could significantly influence the macrofossil composition, but were not able to uniquely explain more than 11.5% of the species composition. Although the macrofossils composition is the driver behind the environmental variables and not the other way around (Heitkonig, 2017). It is impossible to look at the relation that way, without a very long-term experiment.

The von Post is larger when plants are more decomposed (Drzymulska, 2016). Since different plants tissues have different chemical composition and thereby a different degree of decomposition (Drzymulska, 2016), it is likely that the von Post is a good indicator of the plant composition. Additionally, a high decomposition value should be an indicator for a relatively dry mire surface, corresponding to species adapted to dry conditions, while a low decomposition should be an indicator for wetter conditions during peat decomposition for Sphagnum peat (van der Linden & van Geel, 2006). In this study, the von Post is negatively correlated with Sphagna sections and positively with plant species which prefer a drier environment.

The water content and the von Post are independent variables of each other (Figure 10). An explanation why these variables have the strongest relationship with the macrofossils is not very clear and requires more research to come to a conclusion. An explanation why the K_{sat} is not a good predictor of the macrofossils is unknown.

2b) Do the type and surface area of microform patches influence K_{sat} ?

As suggested by the regression analysis, only the type of microform was of importance in predicting the K_{sat} ($P < 0.05$). Small or big microforms do not influence the K_{sat} , which could have been expected, since this will not change the vegetation composition, only the resilience at greater depth possibly.

When another model is used in the regression analysis for the K_{sat} . The minimal size of the microform and the area size of the microform can also be used to predict the K_{sat} (Table 8). When aerial images or remote sensing information is available, size could be used to predict the K_{sat} , especially when other sources of information are available from environmental variables (depth, von Post). This model outcome, that sizes are of influence on the K_{sat} , could be proof of self-regulation if a certain threshold is reached. The minimal length of a microform is a measure of how strong a microform could withstand the other type of microform, whereas the maximal size is apparently not a good measure. Possibly the maximal size is less important if a threshold exists for microforms. The area size connects the minimal size and the type of pattern, since dotted patterns have a different minimal size/area size ratio than for instance string patterns.

Eppinga *et al.* (2009b) stated that differences in K_{sat} may be induced by pattern formation. This relationship is not visible in the best models for the shallow K_{sat} , since there the microform type, minimal size and the area size of a microform influence the K_{sat} . However, pattern type does significantly ($P = 0.007$) explain 2.0% of the macrofossils composition, so there could be an indirect relationship between the pattern type and the K_{sat} , via the macrofossils composition. String patterns have a positive relationship with higher water content and K_{sat} and dotted and maze patterns a negative relationship with K_{sat} (Figure 10). Kellner (2003) stated that: "... hydraulic conductivity depends much on the surface micro relief (hummock/hollows), on the elongation and the thickness of the ridges and strings and the interconnection between hollows and pools (Seppä, 1996)." The elongation and the other features that (Kellner, 2003) describes can be classified as different patterns by (Eppinga *et al.*, 2009b) and confirms a possible relationship between pattern type and the K_{sat} . The study of (Eppinga *et al.*, 2009b) is to the author's knowledge the first to show the effect of pattern type on K_{sat} . However, pattern type could still be an important spatial result of differences in K_{sat} or possibly another property of peat via an indirect link.

5.3. Pedological memory in peatland microforms

Macrofossils can help in determining the similarity of microforms as well act as a measure of microform persistence.

3a) Do large microform have higher similarity than smaller microforms, in terms of macrofossils?

The deviance value for the relatively larger hollows compared to the smaller hollows does show a significant lower value from a depth of 40 cm onwards. This confirms the hypothesis that from this depth onwards the vegetation in the larger hollow microforms changes less than the smaller hollow microforms. For the large hummock, there is not a significant trend over depth, therefore it is impossible to confirm the memory effect for this type of microform. Possibly the *Aulacomnium Palustre* found in large quantities at a depth of 30-40 cm in a big hummock microform results in non-significant values (Figure 15). It is likely that larger microforms have more persistent vegetation, compared to smaller microforms on catchment scale. Thereby confirming higher resilience for larger features, like (Fischer *et al.*, 2006) found in the case with islands for biodiversity.

3b) Do individual cores show pedological memory?

When larger microforms have a higher similarity, site codes with a g (big microform) should switch less from cluster compared to site codes with a k (small microform) (Figure 17). From the cluster dendrogram (Figure 17), it is not clearly visible that the larger microforms switch less often from clusters in relation to the smaller microforms.

The 10 cm depth measurements in the big hollow in site 4 and 5 are in the same cluster. These sites are approximately a kilometer away from each other, separated by a forest and having the same distance to the forest-mire margin. Since the top of the samples are a large hollow, it is expected that the vegetation on 10 cm depth would also represent hollow vegetation. However both samples mainly consist out of *Sphagna* from the *Acutifolia* section, which occupies hummocks (Wieder *et al.*, 2006). Possibly the forest plays a role and made that these sites were much drier in the past, this results in a low pedological memory for these two sites. The big hollow at 10 cm beneath the water level of site 6 also shows more *Sphagna Acutifolia*, whereas the same size, depth and microform in site 1, 2 and 3 are more dominated by *Sphagna Cuspidata*. Caution is advisable when the pedological memory is calculated on the landscape scale, since there can be a lot of variation in a landscape.

The cluster dendrogram does not give a clear distinction between the large and small microforms. Possibly external factors like a forest (or climate) play a larger role. A next step in pedological research could be a quantitative measure for the pedological persistence on a site.

Consequences for peatland development is that a peatland is a heterogeneous landscape. Therefore, it is better not to take a single core for, for instance, paleo-ecological research. But it is advised to take more cores to account for the fact that microforms

change over depth and laterally. Short distances (in the order of several meters) can result in heterogeneity in terms of developmental history and eco-hydrological dynamics in peatlands.

3c) Limitations

Samples may be biased, since 10 cm in the upper part of the profile may represent only a fraction of the 10 cm at the bottom of the profile and could contain a much longer record, timewise. The peat is more compressed at greater depth (Wong *et al.*, 2009) and also older at greater depth (van der Linden *et al.*, 2008) in general. Dating the samples could give an indication of the growing speed of the peat and more importantly, could help determine the memory effect. Without any dates, it is better not to speak of 'memory'; 'resilience' or 'persistence' would be more in place.

Macrofossils are analysed to the greatest detail, resulting in different classes for plant species which fell within larger groups e.g. *Eriophorum vaginatum*. In the data analysis, this was a different group from *Eriophorum* sp. Furthermore, the *Sphagna Palustre* section could have been subdivided to species level, however due to lack in experience, this was not done.

It is important to note that one study site was used. Although the study was extensive in terms of data collection, it would be of great value if other research continues the work done in this report in other sites and helps to gain more knowledge about the processes in peatlands.

6. Conclusion

6.1. K_{sat} gradient over depth and differences between microforms

The results of this study clearly show a gradient over depth and between different microforms for the K_{sat} . The gradient in the upper 75 cm differs the most between the different microforms and becomes more or less constant after that depth. A difference in K_{sat} supports the existence of the different feedback mechanisms that the vegetation on the different microforms has. This supports the theory that microform vegetation has self-regulation abilities in terms of wetness, which result in microform patterns throughout the peatland.

6.2. K_{sat} in relation to other (environmental) variables?

The type of microform (hummock or hollow), the depth of where the sample was taken and the von Post scale are strong and independent controls on the K_{sat} . The bulk density, water content and the relative size of the microform had no effect. Furthermore, the K_{sat} only influences the plant composition for 1.6%. This relationship is very weak and not significant. The von Post explained the variation in the plant composition by 6.8% ($P_{adj.}=0.013$), the water content explained 4.8% ($P_{adj.}=0.013$) and the type of pattern explained 2.5% ($P_{adj.}=0.013$). The best predictor is the type of microform for the K_{sat} measured at 10cm (Table 8). However, when aerial images or other remote sensing data is available, sizes of microforms could be used to predict the K_{sat} . Then the minimal size of the microform and the area of the microform can be used to predict the K_{sat} measured at 10cm, especially in relation to information about the physical measurements.

6.3. Pedological memory in peatland microforms

Whether pedological memory has a direct effect on the K_{sat} is unclear, since the relationship between K_{sat} and macrofossils is not strong. However, the macrofossils can help in determining the similarity of microforms as well act as a measure of pedological memory. The deviance value for the relatively larger hollows compared to the smaller hollows does show a significantly lower value from a depth of 40 cm onwards. This confirms that from this depth onwards the vegetation in the larger hollow microforms changes less than the smaller hollow microforms. For the large hummock microforms, there is no significant trend over depth, therefore it is impossible to confirm the memory effect for this type of microform. Although Figure 12 shows a trend, making it more likely that larger microforms have more consistent vegetation, compared to smaller microforms, possibly confirming higher resilience for larger microforms on catchment scale. The cluster dendrogram shows if vegetation samples from a certain depth are significantly the same or different with other samples (Figure 17). Some samples remain in the same cluster over 3 different depths, this is proof for a high pedological memory for this core e.g. 3gu. On the other hand, some cores fall within multiple clusters, showing low pedological memory e.g. 1gu. Furthermore, large hummocks show large quantities of hollow vegetation at the depth of 10cm below the groundwater level. A cluster dendrogram is a good method to gain overview in combination with a diagnostic diagram about the persistence of a microform.

7. Recommendations

7.1. Data collection in the field

Poor recovery in parts of the cores meant that not all the required depths could be sampled for environmental samples at all depths, duplicate sampling could be a solution to reduce risk of poor recovery. Furthermore, the peat became very impermeable at an average depth of 100cm making the stabilization time long for the K_{sat} measurements. This caused troubles because water was added too soon. However, this report gives more insight in the expected stabilization time via the K_{sat} value published. Furthermore there is evidence that deeper peat can be relatively permeable, it is important that more work is done on estimating the K_{sat} of deeper peat (Baird *et al.*, 2016).

7.2. Macrofossil prediction model

The chemical composition of the peat could be a good predictor of the macrofossils (Botch & Masing, 1979), since there is already a strong link between the chemical composition and pH with the von Post. Maybe a Fourier Transform Infrared analysis on peat samples could give insight in the polysaccharide, lignin-like and aliphatic structures, possibly explaining the increased humification over depth (Artz *et al.*, 2008). The von Post showed good results in predicting the K_{sat} and the macrofossil composition.

7.3. Macrofossil in terms of hummock or hollow ratio

It could have been useful to categorize the macrofossils found in terms of “hollowness” or “hummockness” to see whether a microform changed often in the past. Classifying the macrofossils in terms of “hollowness” and “hummockness” required more knowledge about the wetness indicative property of a plant species.

7.4. Further research

More research is needed to grasp the full extent of the influence that microform size and pattern type can have on the K_{sat} and macrofossil composition. Possibly a meta-analysis of other K_{sat} measurements in a boreal peatland can help to gain more insight in other environmental variables that influence the K_{sat} and possible pattern forming processes. And finally, dating of the samples could have given a lot of insight in the speed of the changes and by including the age of samples in further research, this could give a better view on the pedological memory of peatland.

8. Acknowledgements

I would like to thank the following persons for their collaboration during the fieldwork, lab work and/or data analysis: Jelmer Nijp (WUR) for being a superb - and inspiring supervisor with lots of energy. Marloes Arens (WUR) for helping me in the field and during the analysis of the data. Arnaud Temme (WUR) for the opportunity to join this project. Elisabet Bohlin (SLU) for the training in macrofossil analysis and making me enthusiastic for this type of research. Bas van Geel (UvA) for the second opinion on my macrofossils analysis. Mats Nilsson (SLU) for all the help during the whole fieldwork campaign. Pernilla Löfvenius (SLU) & Thomas Hörnlund (SLU) for all the support in Sweden. Frans Moller (WUR) & Jan van Walsem (WUR) for the equipment I could borrow and for keeping me company in the lab when I was working on the determination of the macrofossils. Jasper van Ruijven (WUR) for statistical advice. And last but not least, my family, friends and girlfriend for their support during the process.

Without all of you, this report would not be there.

References

- Aaviksoo, K., Ilomets, M., & Zobel, M. (1993). Dynamics of mire communities: a Markovian approach (Estonia). *Wetlands and Shallow Continental Water Bodies*, 2, 23-43.
- Alexandersson, H., Karlström, C., & Larsson-McCann, S. (1991). Temperature and precipitation in Sweden 1961-90. Reference normals. *Sveriges Meteorologiska och Hydrologiska Inst.*
- Alm, J., Schulman, L., Walden, J., Nykänen, H., Martikainen, P. J., & Silvola, J. (1999). Carbon balance of a boreal bog during a year with an exceptionally dry summer. *Ecology*, 80(1), 161-174.
- Angstrom, A. (1974). Sveriges Klimat. 3: rd ed. *Generalsta-bens litografiska anstalt, Stockholm.*
- Arens, M. P. (2017). MSc thesis: The effect of spatial organization of peatland patterns on the hydrology. *Unpublished manuscript, Soil Geography and Landscape Group, Wageningen University, Wageningen, The Netherlands.*
- Artz, R. R., Chapman, S. J., Robertson, A. J., Potts, J. M., Laggoun-Défarage, F., Gogo, S., . . . Francez, A.-J. (2008). FTIR spectroscopy can be used as a screening tool for organic matter quality in regenerating cutover peatlands. *Soil Biology and Biochemistry*, 40(2), 515-527.
- Baird, A. J., Milner, A. M., Blundell, A., Swindles, G. T., & Morris, P. J. (2016). Microform-scale variations in peatland permeability and their ecohydrological implications. *Journal of Ecology*.
- Barber, K. E. (1981). *Peat stratigraphy and climatic change*: Balkema.
- Barber, K. E., Chambers, F. M., & Maddy, D. (2003). Holocene palaeoclimates from peat stratigraphy: macrofossil proxy climate records from three oceanic raised bogs in England and Ireland. *Quaternary Science Reviews*, 22(5), 521-539.
- Belyea, L. R., & Baird, A. J. (2006). Beyond "the limits to peat bog growth": cross-scale feedback in peatland development. *Ecological Monographs*, 76(3), 299-322.
- Belyea, L. R., & Clymo, R. (2001). Feedback control of the rate of peat formation. *Proceedings of the Royal Society of London B: Biological Sciences*, 268(1473), 1315-1321.
- Belyea, L. R., & Malmer, N. (2004). Carbon sequestration in peatland: patterns and mechanisms of response to climate change. *Global Change Biology*, 10(7), 1043-1052.
- Boelter, D. H. (1969). Physical properties of peats as related to degree of decomposition. *Soil Science Society of America Journal*, 33(4), 606-609.
- Bohlin, E. (1993). Botanical Composition of Peat : Implications on Chemical, Microbiological and Physical Properties.
- Botch, M., & Masing, V. (1979). *Regionality of mire complex types in the USSR*. Paper presented at the Proceedings of the International Symposium on Classification of Peat and Peatlands.
- Bragazza, L. (2008). A climatic threshold triggers the die-off of peat mosses during an extreme heat wave. *Global Change Biology*, 14(11), 2688-2695.
- Brand, E. W., & Premchitt, J. (1982). Response characteristics of cylindrical piezometers. *Géotechnique*, 32(3), 203-216.
- Branham, J. E., & Strack, M. (2014). Saturated hydraulic conductivity in Sphagnum-dominated peatlands: do microforms matter? *Hydrological Processes*, 28(14), 4352-4362.
- Bridgman, S. D., Pastor, J., Dewey, B., Weltzin, J. F., & Updegraff, K. (2008). Rapid carbon response of peatlands to climate change. *Ecology*, 89(11), 3041-3048.
- Burnham, K. P., & Anderson, D. R. (2003). *Model selection and multimodel inference: a practical information-theoretic approach*: Springer Science & Business Media.
- Chambers, F., Beilman, D., & Yu, Z. (2010). Methods for determining peat humification and for quantifying peat bulk density, organic matter and carbon content for palaeostudies of climate and peatland carbon dynamics. *Mires and Peat*, 7, 7.1-7.10.
- Collins, M., Knutti, R., Arblaster, J., Dufresne, J.-L., Fichet, T., Friedlingstein, P., . . . Krinner, G. (2013a). Long-term climate change: projections, commitments and irreversibility.
- Collins, M., Knutti, R., Arblaster, J., Dufresne, J., Fichet, T., Friedlingstein, P., . . . Krinner, G. (2013b). Climate change 2013: the physical science basis. Contribution of Working Group I to the Fifth Assessment Report of the Intergovernmental Panel on Climate Change. *Long-term Clim. Chang. Proj. Commitments Irreversibility*, Cambridge Univ. Press. Cambridge, UK, New York.
- Couwenberg, J. (2005). A simulation model of mire patterning—revisited. *Ecography*, 28(5), 653-661.
- Couwenberg, J., & Joosten, H. (2005). Self-organization in raised bog patterning: The origin of microtopo zonation and mesotope diversity. *Journal of Ecology*, 93(6), 1238-1248.
- De Vleeschouwer, F., Chambers, F. M., & Swindles, G. T. (2010). Coring and sub-sampling of peatlands for palaeoenvironmental research. *Mires and Peat*, 7.
- Dijk, G., Nijp, J. J., Metselaar, K., Lamers, L. P., & Smolders, A. J. (2017). Salinity-induced increase of the hydraulic conductivity in the hyperheic zone of coastal wetlands. *Hydrological Processes*, 31(4), 880-890.
- Dlugokencky, E., & Tans, P. (2016). Trends in Atmospheric Carbon Dioxide. Retrieved 1-6-2016, 2016, from www.esrl.noaa.gov/gmd/ccgg/trends/
- Drzymulska, D. (2016). Peat decomposition—shaping factors, significance in environmental studies and methods of determination; a literature review. *Geologos*, 22(1), 61-69.
- El-Daoushy, F., Tolonen, K., & Rosenberg, R. (1982). Lead 210 and moss-increment dating of two Finnish Sphagnum hummocks. *Nature*, 296(5856), 429-431.
- Eppinga, M. B., De Ruiter, P. C., Wassen, M. J., & Rietkerk, M. (2009a). Nutrients and hydrology indicate the driving mechanisms of peatland surface patterning. *The American Naturalist*, 173(6), 803-818.
- Eppinga, M. B., Rietkerk, M., Wassen, M. J., & De Ruiter, P. C. (2009b). Linking habitat modification to catastrophic shifts and vegetation patterns in bogs. *Plant Ecology*, 200(1), 53-68.
- Fischer, J., Lindenmayer, D. B., & Manning, A. D. (2006). Biodiversity, ecosystem function, and resilience: ten guiding principles for commodity production landscapes. *Frontiers in Ecology and the Environment*, 4(2), 80-86.
- Frolking, S., & Roulet, N. T. (2007). Holocene radiative forcing impact of northern peatland carbon accumulation and methane emissions. *Global Change Biology*, 13(5), 1079-1088.
- Gorham, E. (1991). Northern Peatlands - Role in the Carbon-Cycle and Probable Responses to Climatic Warming. *Ecological Applications*, 1(2), 182-195. doi: Doi 10.2307/1941811
- Grover, S., & Baldock, J. (2013). The link between peat hydrology and decomposition: Beyond von Post. *Journal of Hydrology*, 479, 130-138.
- Heikurainen, L., & Huikari, O. (1952). The microscopic determination of peat types. *Commun Inst for Fenn*, 40, 1-34.

- Heitkonig, I. (2017). personal communication.
- Hoag, R., & Price, J. (1995). A field-scale, natural gradient solute transport experiment in peat at a Newfoundland blanket bog. *Journal of Hydrology*, 172(1-4), 171-184.
- Holden, J., & Burt, T. (2003). Hydraulic conductivity in upland blanket peat: measurement and variability. *Hydrological Processes*, 17(6), 1227-1237.
- Hossain, M., Chen, W., & Zhang, Y. (2015). Bulk density of mineral and organic soils in the Canada's arctic and sub-arctic. *Information Processing in Agriculture*, 2(3), 183-190.
- Ingram, H. A. P. (1983). A.J.P. Gore (Ed.). *Ecosystems of the World 4A. Mires: Swamp, Bog, Fen and Moor*, Elsevier, Amsterdam (Hydrology), 67-158.
- Ivanov, K. (1975). Water Movement in Mirelands. translated from Russian by A. Thomson and H. A. P. Ingram. Academic: New York.
- Joosten, H., & Clarke, D. (2002). Wise use of mires and peatlands: International mire conservation group.
- Kellner, E. (2003). *Wetlands: Different Types, Their Properties and Functions*: Svensk kärnbränslehantering AB, Swedish Nuclear Fuel and Waste Management Company.
- Laine, J., Harju, P., Timonen, T., Laine, A., Tuittila, E.-S., Minkkinen, K., & Vasander, H. (2009). *The Intricate Beauty of Sphagnum Mosses—a Finnish Guide to Identification*. University of Helsinki, Department of Forest Ecology: FI.
- Larsen, J. A. (2013). *The boreal ecosystem*: Elsevier.
- Lepš, J., & Šmilauer, P. (2003). *Multivariate analysis of ecological data using CANOCO*: Cambridge university press.
- Malmer, N. (1962). *Studies on mire vegetation in the archaean area of southwestern Götaland (South Sweden)*: Distributor: Almqvist and Wiksell.
- Malmer, N., & Wallén, B. (2004). Input rates, decay losses and accumulation rates of carbon in bogs during the last millennium: internal processes and environmental changes. *The Holocene*, 14(1), 111-117.
- Mauquoy, D., & Van Geel, B. (2007). Mire and peat macros. *Encyclopedia of quaternary science*, 3, 2315-2336.
- Moore, P. (1977). Stratigraphy and pollen analysis of Claish Moss, north-west Scotland: significance for the origin of surface-pools and forest history. *The Journal of Ecology*, 375-397.
- Morris, P., Baird, A., & Belyea, L. (2013). The role of hydrological transience in peatland pattern formation. *Earth Surface Dynamics*, 1(1), 29.
- Morris, P. J., Baird, A. J., & Belyea, L. R. (2012). The DigiBog peatland development model 2: ecohydrological simulations in 2D. *Ecohydrology*, 5(3), 256-268.
- Morris, P. J., Baird, A. J., & Belyea, L. R. (2015). Bridging the gap between models and measurements of peat hydraulic conductivity. *Water Resources Research*, 51(7), 5353-5364.
- Nijp, J. J. (2015). Fine scale ecohydrological processes in northern peatlands and their relevance for the carbon cycle.
- Nijp, J. J., Limpens, J., Metselaar, K., Peichl, M., Nilsson, M. B., Zee, S. E., & Berendse, F. (2015). Rain events decrease boreal peatland net CO₂ uptake through reduced light availability. *Global Change Biology*, 21(6), 2309-2320.
- Nijp, J. J., Limpens, J., Metselaar, K., Zee, S. E., Berendse, F., & Robroek, B. J. (2014). Can frequent precipitation moderate the impact of drought on peatmoss carbon uptake in northern peatlands? *New Phytologist*, 203(1), 70-80.
- Nilsson, M., Sagerfors, J., Buffam, I., Laudon, H., Eriksson, T., Grelle, A., . . . Lindroth, A. (2008). Contemporary carbon accumulation in a boreal oligotrophic minerogenic mire—A significant sink after accounting for all C-fluxes. *Global Change Biology*, 14(10), 2317-2332.
- Nimmo, J. (2004). Porosity and pore size distribution. *Encyclopedia of Soils in the Environment*, 3, 295-303.
- Nungesser, M. K. (2003). Modelling microtopography in boreal peatlands: hummocks and hollows. *Ecological Modelling*, 165(2), 175-207.
- Ottosson-Löfvenius, M. (2005). Sammanställning Kulbäcklidens försökspark 2004. *Annual Report. Reference climate monitoring program at the Vindeln experimental forest*. Swedish University of Agricultural Sciences, Umeå, 35.
- Ottosson-Löfvenius, M. (2006). Sammanställning Kulbäcklidens försökspark 2005. *Annual Report. Reference climate monitoring program at the Vindeln experimental forest*. Swedish University of Agricultural Sciences, Umeå, 35.
- Päivänen, J. (1973). *Hydraulic conductivity and water retention in peat soils*: Suomen metsätieteellinen seura.
- Phillips, J. D., & Marion, D. A. (2004). Pedological memory in forest soil development. *Forest Ecology and Management*, 188(1), 363-380.
- Price, J., Heathwaite, A., & Baird, A. (2003). Hydrological processes in abandoned and restored peatlands: an overview of management approaches. *Wetlands Ecology and Management*, 11(1-2), 65-83.
- Ridolfi, L., D'Odorico, P., & Laio, F. (2006). Effect of vegetation–water table feedbacks on the stability and resilience of plant ecosystems. *Water Resources Research*, 42(1).
- Rietkerk, M., Dekker, S., Wassen, M., Verkoost, A., & Bierkens, M. (2004a). A putative mechanism for bog patterning. *The American Naturalist*, 163(5), 699-708.
- Rietkerk, M., Dekker, S. C., de Ruiter, P. C., & van de Koppel, J. (2004b). Self-organized patchiness and catastrophic shifts in ecosystems. *Science*, 305(5692), 1926-1929.
- Rietkerk, M., & van de Koppel, J. (1997). Alternate stable states and threshold effects in semi-arid grazing systems. *Oikos*, 69-76.
- Rydin, H., Jeglum, J. K., & Jeglum, J. K. (2013). *The biology of peatlands*, 2e: Oxford university press.
- Scheffer, M., Carpenter, S., Foley, J. A., Folke, C., & Walker, B. (2001). Catastrophic shifts in ecosystems. *Nature*, 413(6856), 591-596.
- Scheffer, M., & Carpenter, S. R. (2003). Catastrophic regime shifts in ecosystems: linking theory to observation. *Trends in ecology & evolution*, 18(12), 648-656.
- Seppä, H. (1996). The morphological features of the Finnish peatlands. *Peatlands in Finland*, 27-33.
- Smith, A. J. E., & Smith, R. (2004). *The moss flora of Britain and Ireland*: Cambridge University Press.
- Swanson, D. K., & Grigal, D. F. (1988). A simulation model of mire patterning. *Oikos*, 309-314.
- Team, R. C. (2014). R: A language and environment for statistical computing. Vienna, Austria: R Foundation for Statistical Computing; 2014.
- van der Linden, M., Barke, J., Vickery, E., Charman, D. J., & van Geel, B. (2008). Late Holocene human impact and climate change recorded in a North Swedish peat deposit. *Palaeogeography, Palaeoclimatology, Palaeoecology*, 258(1), 1-27.
- van der Linden, M., & van Geel, B. (2006). Late Holocene climate change and human impact recorded in a south Swedish ombrotrophic peat bog. *Palaeogeography, Palaeoclimatology, Palaeoecology*, 240(3), 649-667.
- von Post, L. (1922). Sveriges Geologiska Undersöknings torvinventering och några av dess hittills vunna resultat.
- Walker, D., & Walker, P. (1961). Stratigraphic evidence of regeneration in some Irish bogs. *The Journal of Ecology*, 169-185.
- Whittington, P., Strack, M., Van Haarlem, R., Kaufman, S., Stoesser, P., Maltez, J., . . . Stone, M. (2007). The influence of peat volume change and vegetation on the hydrology of a kettle-hole wetland in Southern Ontario, Canada. *Mires and Peat*, 2(9), 1-14.

- Wieder, R. K. (2001). PAST, PRESENT, AND FUTURE PEATLAND CARBON BALANCE: AN EMPIRICAL MODEL BASED ON ²¹⁰Pb-DATED CORES. *Ecological Applications*, 11(2), 327-342.
- Wieder, R. K., Vitt, D. H., & Benscoter, B. W. (2006). Peatlands and the boreal forest *Boreal peatland ecosystems* (pp. 1-8): Springer.
- Wong, L., Hashim, R., & Ali, F. (2009). A review on hydraulic conductivity and compressibility of peat. *Journal of Applied Sciences*, 9(18), 3207-3218.
- Yu, Z., Loisel, J., Brosseau, D. P., Beilman, D. W., & Hunt, S. J. (2010). Global peatland dynamics since the Last Glacial Maximum. *Geophysical Research Letters*, 37(13).
- Zlotnik, V. A., Goss, D., & Duffield, G. M. (2010). General Steady-State Shape Factor for a Partially Penetrating Well. *Ground water*, 48(1), 111-116.

Appendix

Remarks and copyright images

Due to poor recovery and visual differences in the samples. The following samples were not taken from the first two cms but from different depths for the bulk density data and the water content data. 1go108-110, 1go100-102, 4ku18-20, 5ko108-20, 1go10-20, 1ko100-102, 1ko108-110, 1gu18-20, 4ku18-20, 1ku10-12, 1ku18-20 (the last numbers indicate the depth (cm) in respect to the lowest summer groundwater level).

The source of the image on the left in figure 1 is from: <http://www.jansvenungsson.com/pics2/pms66/23.gif>. The owner of the cover photo is Jelmer Nijp (WUR).

Pycnometer table

Table 9. Pycnometer data

Site code	Depth (cm)	Volume 1 (cm ³)	Volume 2 (cm ³)	Volume 3 (cm ³)	Average volume (cm ³)	Volume of the soil (cm ³)	dry weight (g)	Von Post (-)	particle density (g/cm ³)	bulk density (g/cm ³)	solid fraction (%)	Porosity (-)
1Go	15	22	21	21	21.3	1.666667	1.694	1	1.0164	0.021302	2.095868	98.90413
4Ko	15	22	21	21	21.3	1.666667	0.5763	3	0.34578	0.036235	10.47934	89.52066
6Ku	15	21	21	21	21	1.333333	1.5461	5	1.159575	0.097213	8.38347	91.61653
5Gu	15	20	20	21	20.3	0.666667	1.0434	9	1.5651	0.065605	4.191735	95.80826
1Gu	15	21	22	21	21.3	1.666667	0.957	3	0.5742	0.060172	10.47934	89.52066
1Go	35	22	21	20	21	1.333333	1.0127	1	0.759525	0.063675	8.38347	91.61653
6Ko	35	21	21	21	21	1.333333	1.1111	6	0.833325	0.056104	6.732581	93.26742
3Gu	35	20	20	20	20	0.333333	0.1866	2	0.5598	0.011733	2.095868	97.90413
1Gu	35	21	21	22	21.3	1.666667	1.192	6	0.7152	0.074948	10.47934	89.52066
5Gu	35	21	21	21	21	1.333333	0.7841	3	0.588075	0.049301	8.38347	91.61653
6Gu	35	21	21	21	21	1.333333	1.4687	8	1.101525	0.092346	8.38347	91.61653

Diagnostic diagram of the macrofossils after cluster analysis

Table 10. Diagnostic diagram of cluster in Figure 17. Count data of the following Species/plant sections per site and depth (last 2,3 digits of site code): Ac= Sph. Acutifolia, Pa= Sph. Palustre, Cu = Sph. Cuspidata, un_sp=unidentified Sph., tot_sp= Total Sph., Po = *Polytrichum sp.*, B=brown mosses, Nroot=Ericaceous roots, Nbark=Ericaceous bark, Lig = trees and shrubs, Er_vag= *Eriophorum vag.*, C=*Cyperaceae sp.*, ER=*Eriophorum sp.*, Cl=*Carex limosa*, Cb=*Carex sp.*, Dre=*Drepanocladus sp.*, R.A.=*Rhynchospora alba*, S.p.=*Scheuchzeria palustris*, A.P.=*Aulacomnium palustre*, S.C.=*Scirpus cespitosus*, unkn=unknown fragments.

Sitecode	Ac	Pa	Cu	Unid.sp	Pol	Brown	Nroot	Nbark	Lig	Er_vag	Cyp	Er	Cl	Cb	Dre	R.A.	S.P.	A.P.	S.C.	unkn	Cluster
3gu60	8	6	31	1	1	3	12	1	0	0	9	7	0	0	21	0	0	1	0	0	1
4go100	2	11	17	0	0	3	14	2	0	1	16	1	0	4	26	1	3	0	0	0	1
3gu150	4	0	31	0	0	6	23	6	2	3	10	11	0	0	2	0	0	0	0	1	1
4ku60	12	5	26	2	2	1	23	1	0	6	7	13	0	0	3	0	0	0	0	0	1
2go100	13	14	28	1	0	0	38	1	0	0	4	1	0	0	0	0	0	0	0	1	1
3gu100	8	0	16	0	1	5	34	5	3	0	19	2	0	0	3	0	1	0	0	4	1
3ko60	1	0	9	0	1	1	21	12	10	3	5	36	1	0	0	0	0	0	0	0	2
5ko100	6	0	14	0	0	0	28	2	7	8	2	33	0	0	0	0	0	0	0	0	2
5gu30	18	0	7	0	0	0	42	3	6	11	3	11	0	0	0	0	0	0	0	0	3
5ko10	14	2	6	1	0	3	32	4	3	11	7	15	0	0	0	0	0	0	0	3	3
2ku30	29	2	1	0	0	1	37	3	3	6	4	14	0	0	0	0	0	0	0	2	3
5gu100	23	3	10	0	0	0	34	1	3	8	8	2	0	0	0	0	2	0	0	5	3
4ku30	19	4	14	2	0	6	19	1	1	12	11	10	0	0	0	0	0	0	0	1	4
1gu100	32	3	14	1	0	0	20	1	1	9	5	16	0	0	0	0	0	0	0	0	4
2ku60	24	3	20	0	0	0	16	1	1	16	0	20	0	0	0	0	0	0	0	0	4
5go60	24	1	15	0	0	0	22	3	0	12	1	23	0	0	0	0	0	0	0	0	4
2ko10	21	0	78	0	0	0	1	0	0	0	0	0	0	0	0	0	0	0	0	0	5
3ko10	19	0	74	1	0	0	1	0	0	0	3	1	0	0	0	0	0	0	0	2	5
3ko30	20	0	53	2	0	1	10	0	0	5	2	7	0	1	0	0	0	0	1	0	5
1ko30	27	2	65	0	0	0	2	4	0	0	0	0	0	0	0	0	0	0	0	0	5
2go30	23	0	66	0	0	0	9	0	0	0	2	0	0	0	0	0	0	0	0	0	5
1go60	11	8	64	1	0	1	8	0	0	5	1	2	0	0	0	0	0	0	0	0	6
1ko100	2	3	89	3	0	0	0	0	0	0	0	3	0	0	0	0	0	0	0	1	6
3go10	5	0	90	0	0	0	5	1	0	0	0	0	0	0	0	0	0	0	0	0	6
1go100	11	2	78	2	0	0	6	0	2	0	0	0	0	0	1	0	0	0	0	0	6

3go30	10	0	85	1	0	0	4	0	0	0	0	0	0	0	0	0	0	0	0	6
1gu60	36	18	37	0	0	0	7	0	0	0	1	1	0	0	0	0	0	0	1	7
5gu10	37	12	38	0	0	0	8	0	0	0	3	2	0	0	0	0	0	0	0	7
1ko60	49	16	33	1	0	0	1	0	0	0	0	1	0	0	0	0	0	0	0	7
1gu10	44	14	31	0	0	0	8	1	0	2	0	0	0	0	0	0	0	0	0	7
2gu30	43	12	35	0	1	0	8	0	0	0	0	0	0	0	0	0	0	0	0	7
2ko60	57	3	28	1	0	0	7	0	0	2	1	1	0	0	0	0	0	0	0	7
6go10	46	5	26	0	0	1	4	1	0	9	2	6	0	0	0	0	0	0	1	7
6go60	42	5	28	0	0	0	12	5	0	1	7	0	0	0	0	0	0	0	0	7
6gu10	35	5	28	4	1	0	11	3	1	2	3	7	0	0	0	0	0	0	1	7
5gu60	43	7	36	0	1	0	8	3	1	0	2	0	0	0	0	0	0	0	0	7
6ku60	42	1	38	2	0	0	11	4	0	0	0	2	0	0	0	0	0	0	0	7
2go60	30	1	35	5	0	0	23	0	1	0	4	0	0	0	0	0	0	0	2	7
4gu60	31	6	31	0	0	0	21	3	0	3	1	4	0	0	0	0	0	0	0	7
4gu100	36	3	36	0	0	1	18	0	1	4	1	1	0	0	0	0	0	0	1	7
5ku100	35	2	33	1	0	0	17	1	1	3	1	6	0	0	0	0	0	0	1	7
4ko30	36	5	40	2	6	4	2	0	0	0	0	3	0	0	0	0	0	0	3	7
1go30	38	8	53	0	0	0	0	0	0	0	0	0	0	0	1	0	0	0	0	7
2go10	38	0	61	0	0	0	0	0	0	0	0	1	0	0	0	0	0	0	0	7
2ko30	41	0	56	0	0	0	1	0	0	0	1	2	0	0	0	0	0	0	0	7
5ko60	37	3	43	2	0	0	9	1	0	0	5	0	0	0	0	0	0	0	0	7
4ku100	38	8	42	1	0	0	8	1	0	1	2	0	0	0	0	0	0	0	0	7
6go30	43	4	43	0	0	0	7	1	0	0	1	1	0	0	0	0	0	0	0	7
1ku10	33	6	36	0	0	0	11	0	0	1	2	10	0	0	0	0	0	0	1	7
4ko60	29	11	38	1	0	0	12	2	0	3	4	1	0	0	0	0	0	0	0	7
4ku10	30	7	38	0	1	2	12	1	0	0	2	3	0	1	3	0	0	0	1	7
1ku60	20	27	29	0	0	0	18	0	0	1	2	3	0	0	0	0	0	0	0	8
4ku100	10	29	19	0	2	0	19	2	6	0	2	2	0	3	6	0	0	0	0	8
2ko100	10	32	19	0	0	1	17	0	0	2	10	9	0	0	0	0	0	0	0	8
4go30	11	35	14	0	0	2	19	1	0	0	15	0	1	0	1	0	0	0	1	8

1ku100	19	50	6	0	0	0	16	0	0	0	6	3	0	0	0	0	0	0	0	8
4go60	20	29	11	2	2	2	19	3	0	0	4	6	0	0	2	0	0	0	0	8
4gu30	45	15	23	0	0	0	8	0	0	0	7	2	0	0	0	0	0	0	0	9
6ko10	39	17	24	0	0	0	10	3	1	1	1	2	0	0	0	0	2	0	0	9
6ko30	41	20	25	0	0	0	6	4	0	1	1	1	0	0	0	0	0	0	0	9
6ku30	32	28	23	2	0	0	12	1	0	0	1	1	0	0	0	0	1	0	0	10
2gu60	38	22	28	1	0	0	6	0	3	0	2	0	0	0	0	0	0	0	0	10
4ko10	34	22	27	1	0	0	11	0	0	0	4	0	0	0	0	0	0	0	0	10
6ko60	35	7	7	1	0	1	30	12	1	0	0	4	0	0	0	0	0	0	0	11
2ku10	43	6	4	5	2	6	32	2	0	0	0	0	0	0	2	0	0	0	0	11
4gu10	38	7	3	2	2	7	23	4	1	3	3	3	0	0	4	0	0	0	0	11
2gu100	34	2	11	1	1	0	15	2	1	8	0	12	0	0	15	0	0	0	0	11
5go30	40	1	13	0	0	0	34	1	0	4	0	7	0	0	0	0	0	0	0	11
1ku30	33	6	21	2	0	0	22	0	5	2	2	5	0	0	0	0	0	0	0	11
5go100	31	2	19	0	0	0	27	5	5	3	0	9	0	0	0	0	0	0	0	11
4go10	44	7	13	1	0	1	11	1	1	0	17	6	0	0	0	0	0	0	0	12
5go10	52	14	11	0	0	0	9	1	0	2	8	5	0	0	0	0	0	0	0	12
2ku100	26	18	15	2	0	0	20	4	1	1	0	10	0	0	3	0	0	0	0	13
5ku60	28	7	19	0	0	1	21	4	1	4	13	0	0	0	0	0	0	0	1	13
2gu10	41	13	19	0	0	0	21	1	0	0	1	0	0	0	4	0	0	0	0	13
1gu30	34	16	24	1	0	0	18	2	0	0	6	0	0	0	0	0	0	0	0	13
6ku10	39	9	27	1	0	0	20	2	0	1	1	0	0	0	0	0	0	0	0	13
1go10	10	20	51	2	0	0	2	1	0	0	0	0	6	7	0	0	0	0	0	-
1ko10	53	26	19	0	0	0	1	1	0	0	0	0	0	0	0	0	0	0	0	-
3ku30	0	0	1	0	0	1	25	10	15	13	18	18	0	0	0	0	0	0	0	-
3ku60	0	1	4	0	0	0	56	10	12	0	9	8	0	0	0	0	0	0	0	-
5ku30	2	0	0	0	0	0	40	0	1	14	11	32	0	0	0	0	0	0	0	-
3go100	3	2	14	0	0	1	23	6	35	0	8	4	0	0	0	0	0	0	1	-
3ku10	4	6	1	0	15	0	30	4	0	3	24	11	0	0	0	0	0	0	0	-
3gu30	6	0	0	0	1	7	19	1	0	0	3	0	0	0	10	0	0	53	0	-

5ko30	10	0	1	1	0	0	19	1	6	24	4	35	0	0	0	0	0	0	0	0	-
3ko100	11	26	2	2	0	0	28	11	7	1	8	0	0	0	0	1	0	0	0	3	-
3ku100	13	4	4	0	1	2	41	3	11	1	7	6	0	0	4	0	0	0	0	4	-
6gu60	13	0	9	1	0	1	20	18	2	24	2	10	0	0	0	0	0	0	0	0	-
6gu30	39	20	15	1	2	3	2	3	0	2	1	13	0	0	0	0	0	0	0	0	-

Reference measurements for the K_{sat} correction

The groundwater level is averaged per day. The groundwater level is plotted below surface. There was no selection on the K_{sat} values, all the data was taken into consideration for this calculation.

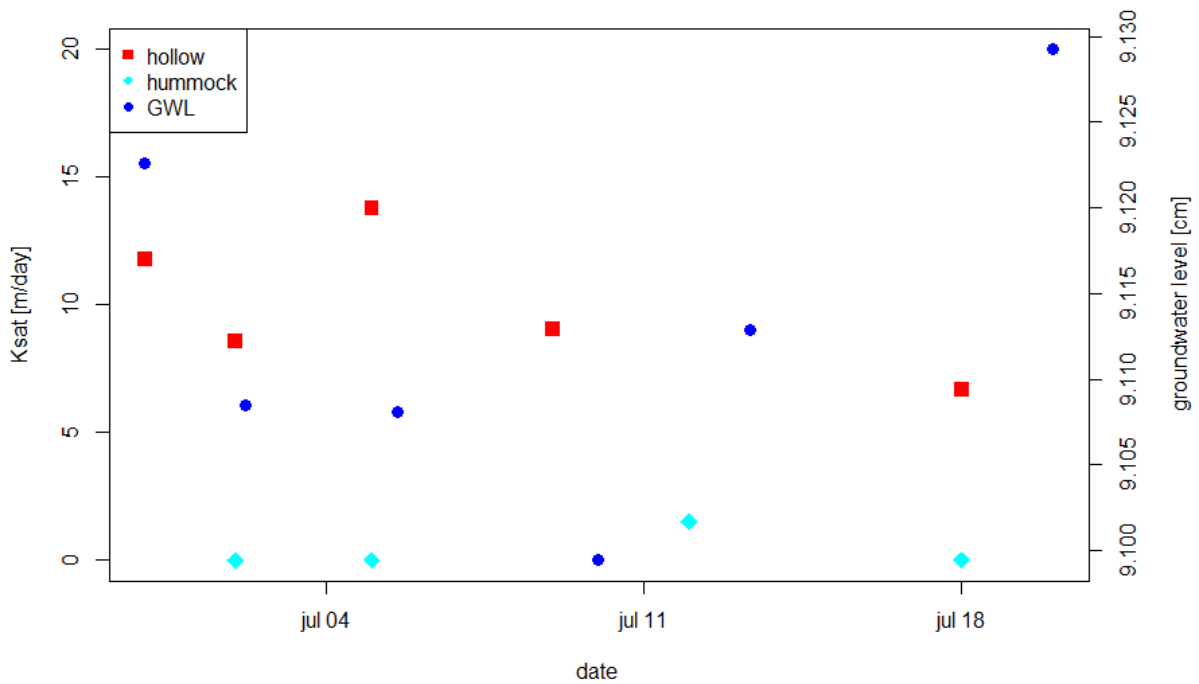


Figure 18. Graphs with K_{sat} and GWL over time. The red and cyan represent the groundwater K_{sat} measurements for the different microforms. Whereas the blue circles represent the ground water levels. All the data is from the reference measurements taken. At the same depth.

Parameters for the deviance values of the microform types

Table 11. The site code, the Manhattan deviance value in respect to the shallowest macrofossil analysis of the site.

Site abbreviation	Deviance value	Site abbreviation	Deviance value
go010	0	ko010	0
go030	51.8	ko030	60.0
go060	71.4	ko060	92.8
go100	109	ko100	116
gu010	0	ku010	0
gu030	71.6	ku030	66.2
gu060	53.8	ku060	76.2
gu100	67.0	ku100	92.7

Table 12. Value for A and B in eq. 11. The standard error, t value and significance based on the measurement in the large hollows (GO).

Parameter	Estimate	Std. Error	t value	Pr(> t)
A	104	10.5	9.93	0.0100
B	105	16.9	6.21	0.0250

Table 13. Value for A and B in eq. 11. The standard error, t value and significance based on the measurement in the large hummocks (GU).

Parameter	Estimate	Std. Error	t value	Pr(> t)
A	61.5	31.7	1.94	0.192
B	48.1	51.0	0.942	0.446

Table 14. Value for A and B in eq. 11. The standard error, t value and significance based on the measurement in the small hollows (KO).

Parameter	Estimate	Std. Error	t value	Pr(> t)
A	117	3.44	34.0	0.000866
B	115	5.52	20.8	0.00230

Table 15. Value for A and B in eq. 11. The standard error, t value and significance based on the measurement in the small hummocks (KU).

Parameter	Estimate	Std. Error	t value	Pr(> t)
A	90.8	17.1	5.33	0.0335
B	83.3	27.4	3.04	0.0934

PCA and RDA analyses

Analysis 'Unconstrained-suppl-vars for figure 9'

Method: **PCA with supplementary variables**

Total variation is 1995.000, supplementary variables account for 22.4%

(adjusted explained variation is 11.1%)

Summary Table:

Statistic	Axis 1	Axis 2	Axis 3	Axis 4
Eigenvalues	0.2086	0.1202	0.0843	0.0788
Explained variation (cumulative)	20.86	32.88	41.32	49.20
Pseudo-canonical correlation (suppl.)	0.6881	0.4455	0.5303	0.2670

Analysis 'Constrained for figure 10'

Method: **RDA**

Total variation is 1995.000, explanatory variables account for 15.7%

(adjusted explained variation is 11.9%)

Summary Table:

Statistic	Axis 1	Axis 2	Axis 3	Axis 4
Eigenvalues	0.0961	0.0356	0.0150	0.0102
Explained variation (cumulative)	9.61	13.17	14.67	15.69
Pseudo-canonical correlation	0.6936	0.6734	0.4939	0.4584
Explained fitted variation (cumulative)	61.29	83.97	93.50	100.00

Analysis 'Constrained'

Forward Selection Results:

Name	Explains %	Contribution %	pseudo-F	P	P(adj)
vPost	6.8	30.4	6.8	0.001	0.013
wc	4.8	21.5	5.0	0.001	0.013
type_pat.string	2.5	11.0	2.6	0.001	0.013
K_zlotnik	1.6	7.1	1.7	0.089	1.

Analysis 'Unconstrained-suppl-vars for figure 10'

Method: **PCA with supplementary variables**

Total variation is 1995.000, supplementary variables account for 16.2%

(adjusted explained variation is 11.5%)

Summary Table:

Statistic	Axis 1	Axis 2	Axis 3	Axis 4
Eigenvalues	0.2086	0.1202	0.0843	0.0788
Explained variation (cumulative)	20.86	32.88	41.32	49.20
Pseudo-canonical correlation (suppl.)	0.6614	0.2542	0.4510	0.1589

Correlation data

		K_zlotnik	vPost	wc
Ac	Pearson Correlation	,167	-,148	,128
	Sig. (2-tailed)	,106	,153	,217
	N	95	95	95
Pa	Pearson Correlation	,025	,037	,065
	Sig. (2-tailed)	,813	,721	,534
	N	95	95	95
Cu	Pearson Correlation	,134	-,480**	,297**
	Sig. (2-tailed)	,197	,000	,003
	N	95	95	95
un_sp	Pearson Correlation	-,089	-,033	,184
	Sig. (2-tailed)	,391	,752	,074
	N	95	95	95
tot_sp	Pearson Correlation	,187	-,410**	,307**
	Sig. (2-tailed)	,069	,000	,003
	N	95	95	95
Po	Pearson Correlation	,261*	-,002	-,067
	Sig. (2-tailed)	,011	,986	,522
	N	95	95	95
B	Pearson Correlation	-,118	-,109	-,360**
	Sig. (2-tailed)	,254	,293	,000
	N	95	95	95
Nroot	Pearson Correlation	-,234*	,429**	-,203*
	Sig. (2-tailed)	,023	,000	,048
	N	95	95	95
Nbark	Pearson Correlation	-,145	,411**	-,062

	Sig. (2-tailed)	,162	,000	,550
	N	95	95	95
L	Pearson Correlation	-,140	,381**	-,151
	Sig. (2-tailed)	,175	,000	,143
	N	95	95	95
Er_vag	Pearson Correlation	-,044	,337**	-,010
	Sig. (2-tailed)	,675	,001	,921
	N	95	95	95
C	Pearson Correlation	,168	,206*	-,225*
	Sig. (2-tailed)	,104	,045	,029
	N	95	95	95
ER	Pearson Correlation	-,088	,457**	-,107
	Sig. (2-tailed)	,395	,000	,301
	N	95	95	95
CI	Pearson Correlation	,090	-,185	,250*
	Sig. (2-tailed)	,387	,072	,015
	N	95	95	95
Cb	Pearson Correlation	,063	-,147	,178
	Sig. (2-tailed)	,546	,156	,084
	N	95	95	95
Dre	Pearson Correlation	-,111	-,020	-,393**
	Sig. (2-tailed)	,285	,844	,000
	N	95	95	95
RA	Pearson Correlation	-,058	,111	,042
	Sig. (2-tailed)	,579	,285	,688
	N	95	95	95
SP	Pearson Correlation	-,022	,059	-,054
	Sig. (2-tailed)	,833	,570	,600
	N	95	95	95
AP	Pearson Correlation	-,031	-,158	-,461**
	Sig. (2-tailed)	,768	,126	,000
	N	95	95	95
SC	Pearson Correlation	,042	,102	-,124
	Sig. (2-tailed)	,688	,323	,232
	N	95	95	95
unkn	Pearson Correlation	-,086	,156	,027
	Sig. (2-tailed)	,408	,131	,796
	N	95	95	95

** . Correlation is significant at the 0.01 level (2-tailed).

* . Correlation is significant at the 0.05 level (2-tailed).

Correlations

		depth	Ksat (zlotnik)	V. Post	Pb	wc	Min size	Max size	Area size	Perim size	est size	cluster
Depth	Pearson Correlation	1	-,389**	,436**	,248*	,159	-,082	,063	-,024	,040	,002	-,165
	Sig. (2-tailed)		,000	,000	,015	,125	,428	,543	,817	,701	,983	,138
	N	95	95	95	95	95	95	95	95	95	95	82
K_zlotnik	Pearson Correlation	-,389**	1	-,430**	-,134	-,126	,204*	,007	,231*	,064	,100	,096
	Sig. (2-tailed)	,000		,000	,194	,225	,047	,945	,024	,536	,333	,392
	N	95	95	95	95	95	95	95	95	95	95	82
vPost	Pearson Correlation	,436**	-,430**	1	,545**	,025	-,025	-,303**	-,169	-,270**	-,156	-,038
	Sig. (2-tailed)	,000	,000		,000	,810	,808	,003	,101	,008	,131	,736
	N	95	95	95	95	95	95	95	95	95	95	82
Pb	Pearson Correlation	,248*	-,134	,545**	1	,188	-,046	-,142	-,133	-,137	-,099	,033
	Sig. (2-tailed)	,015	,194	,000		,068	,660	,168	,199	,187	,339	,766
	N	95	95	95	95	95	95	95	95	95	95	82
Wc	Pearson Correlation	,159	-,126	,025	,188	1	-,082	,285**	,009	,170	-,053	-,007
	Sig. (2-tailed)	,125	,225	,810	,068		,432	,005	,932	,101	,611	,953
	N	95	95	95	95	95	95	95	95	95	95	82
min_size	Pearson Correlation	-,082	,204*	-,025	-,046	-,082	1	,324**	,921**	,529**	,431**	-,019
	Sig. (2-tailed)	,428	,047	,808	,660	,432		,001	,000	,000	,000	,864
	N	95	95	95	95	95	95	95	95	95	95	82
max_size	Pearson Correlation	,063	,007	-,303**	-,142	,285**	,324**	1	,489**	,926**	,274**	,118
	Sig. (2-tailed)	,543	,945	,003	,168	,005	,001		,000	,000	,007	,290
	N	95	95	95	95	95	95	95	95	95	95	82
area_size	Pearson Correlation	-,024	,231*	-,169	-,133	,009	,921**	,489**	1	,659**	,336**	-,011
	Sig. (2-tailed)											
	N											

	Sig. (2-tailed)	,817	,024	,101	,199	,932	,000	,000		,000	,001	,925
	N	95	95	95	95	95	95	95	95	95	95	82
perim_size	Pearson Correlation	,040	,064	-,270**	-,137	,170	,529**	,926**	,659**	1	,335**	,089
	Sig. (2-tailed)	,701	,536	,008	,187	,101	,000	,000	,000		,001	,425
	N	95	95	95	95	95	95	95	95	95	95	82
est_size	Pearson Correlation	,002	,100	-,156	-,099	-,053	,431**	,274**	,336**	,335**	1	-,076
	Sig. (2-tailed)	,983	,333	,131	,339	,611	,000	,007	,001	,001		,498
	N	95	95	95	95	95	95	95	95	95	95	82
cluster	Pearson Correlation	-,165	,096	-,038	,033	-,007	-,019	,118	-,011	,089	-,076	1
	Sig. (2-tailed)	,138	,392	,736	,766	,953	,864	,290	,925	,425	,498	
	N	82	82	82	82	82	82	82	82	82	82	82

** . Correlation is significant at the 0.01 level (2-tailed).

* . Correlation is significant at the 0.05 level (2-tailed).

Correlations

		Ac	Pa	Cu	tot_sp	un_sp
Ac	Pearson Correlation	1	,182	,139	,678**	,104
	Sig. (2-tailed)		,078	,178	,000	,314
	N	95	95	95	95	95
Pa	Pearson Correlation	,182	1	-,129	,325**	,030
	Sig. (2-tailed)	,078		,211	,001	,773
	N	95	95	95	95	95
Cu	Pearson Correlation	,139	-,129	1	,752**	,090
	Sig. (2-tailed)	,178	,211		,000	,388
	N	95	95	95	95	95
tot_sp	Pearson Correlation	,678**	,325**	,752**	1	,161
	Sig. (2-tailed)	,000	,001	,000		,120
	N	95	95	95	95	95
un_sp	Pearson Correlation	,104	,030	,090	,161	1
	Sig. (2-tailed)	,314	,773	,388	,120	
	N	95	95	95	95	95

** . Correlation is significant at the 0.01 level (2-tailed).

Correlations

		Cl	Cb
Cl	Pearson Correlation	1	,809**
	Sig. (2-tailed)		,000
	N	95	95
Cb	Pearson Correlation	,809**	1
	Sig. (2-tailed)	,000	
	N	95	95

** . Correlation is significant at the 0.01 level (2-tailed).

Correlations

		Nroot	Nbark
Nroot	Pearson Correlation	1	,435**
	Sig. (2-tailed)		,000
	N	95	95
Nbark	Pearson Correlation	,435**	1
	Sig. (2-tailed)	,000	
	N	95	95

** . Correlation is significant at the 0.01 level (2-tailed).

Correlations

		Er_vag	ER	C
Er_vag	Pearson Correlation	1	,693**	,153
	Sig. (2-tailed)		,000	,138
	N	95	95	95
ER	Pearson Correlation	,693**	1	,211*
	Sig. (2-tailed)	,000		,040
	N	95	95	95
C	Pearson Correlation	,153	,211*	1
	Sig. (2-tailed)	,138	,040	
	N	95	95	95

** . Correlation is significant at the 0.01 level (2-tailed).

* . Correlation is significant at the 0.05 level (2-tailed).

Correlations

		K_zlotnik	Nroot	depth	vPost	min_size	area_size
K_zlotnik	Pearson Correlation	1	-,234*	-,389**	-,430**	,204*	,231*
	Sig. (2-tailed)		,023	,000	,000	,047	,024
	N	95	95	95	95	95	95
Nroot	Pearson Correlation	-,234*	1	,191	,429**	-,173	-,257*
	Sig. (2-tailed)	,023		,064	,000	,093	,012
	N	95	95	95	95	95	95
depth	Pearson Correlation	-,389**	,191	1	,436**	-,082	-,024
	Sig. (2-tailed)	,000	,064		,000	,428	,817
	N	95	95	95	95	95	95
vPost	Pearson Correlation	-,430**	,429**	,436**	1	-,025	-,169
	Sig. (2-tailed)	,000	,000	,000		,808	,101
	N	95	95	95	95	95	95
min_size	Pearson Correlation	,204*	-,173	-,082	-,025	1	,921**
	Sig. (2-tailed)	,047	,093	,428	,808		,000
	N	95	95	95	95	95	95
area_size	Pearson Correlation	,231*	-,257*	-,024	-,169	,921**	1
	Sig. (2-tailed)	,024	,012	,817	,101	,000	
	N	95	95	95	95	95	95

*. Correlation is significant at the 0.05 level (2-tailed).

** . Correlation is significant at the 0.01 level (2-tailed).